

# An integrated model of soil, hydrology, and vegetation for carbon dynamics in wetland ecosystems

Yu Zhang<sup>1</sup> and Changsheng Li

Complex Systems Research Center, Institute for the Study of Earth, Ocean and Space, University of New Hampshire, Durham, New Hampshire, USA

Carl C. Trettin and Harbin Li

Center for Forested Wetlands Research, USDA Forest Service, Charleston, South Carolina, USA

Ge Sun

Southern Global Change Program, North Carolina State University, Raleigh, North Carolina, USA

Received 26 November 2001; revised 10 May 2002; accepted 16 May 2002; published 19 October 2002.

[1] Wetland ecosystems are an important component in global carbon (C) cycles and may exert a large influence on global climate change. Predictions of C dynamics require us to consider interactions among many critical factors of soil, hydrology, and vegetation. However, few such integrated C models exist for wetland ecosystems. In this paper, we report a simulation model, Wetland-DNDC, for C dynamics and methane (CH<sub>4</sub>) emissions in wetland ecosystems. The general structure of Wetland-DNDC was adopted from PnET-N-DNDC, a process-oriented biogeochemical model that simulates C and N dynamics in upland forest ecosystems. Several new functions and algorithms were developed for Wetland-DNDC to capture the unique features of wetland ecosystems, such as water table dynamics, growth of mosses and herbaceous plants, and soil biogeochemical processes under anaerobic conditions. The model has been validated against various observations from three wetland sites in Northern America. The validation results are in agreement with the measurements of water table dynamics, soil temperature, CH<sub>4</sub> fluxes, net ecosystem productivity (NEP), and annual C budgets. Sensitivity analysis indicates that the most critical input factors for C dynamics in the wetland ecosystems are air temperature, water outflow parameters, initial soil C content, and plant photosynthesis capacity. NEP and CH<sub>4</sub> emissions are sensitive to most of the tested input variables. By integrating the primary drivers of climate, hydrology, soil and vegetation, the Wetland-DNDC model is capable of predicting C biogeochemical cycles in wetland ecosystems. *INDEX TERMS*: 1615 Global Change: Biogeochemical processes (4805); 1890 Hydrology: Wetlands; *KEYWORDS*: wetland, model, carbon cycles, methane emissions, hydrology

**Citation:** Zhang, Y., C. Li, C. C. Trettin, H. Li, and G. Sun, An integrated model of soil, hydrology, and vegetation for carbon dynamics in wetland ecosystems, *Global Biogeochem. Cycles*, 16(4), 1061, doi:10.1029/2001GB001838, 2002.

## 1. Introduction

[2] Wetlands are an important component of the terrestrial landscapes that exert a great influence over global carbon (C) cycle and climate change. Wetlands contain 15–22% of the global terrestrial carbon [Eswaran *et al.*, 1995; Gorham, 1991] and contribute 15–20% of the global methane (CH<sub>4</sub>) emissions to the atmosphere [Aselmann and Crutzen, 1989; Matthews and Fung, 1987]. Wetland ecosystems have

unique characteristics affecting C dynamics. For example, the high water table and its fluctuation are the primary factors driving soil organic carbon (SOC) decomposition [Moore and Dalva, 1997; DeBusk and Reddy, 1988], plant C fixation [Bubier, 1995], CH<sub>4</sub> production and consumption [Moore and Roulet, 1993; Bellisario *et al.*, 1999], and other biogeochemical processes in the wetlands. Small changes in water table or temperature can perturb the C balance in the peatlands due to alterations in soil organic matter decomposition and/or plant production [Bubier *et al.*, 1998; Silvola *et al.*, 1996; Shurpali *et al.*, 1995]. Accordingly, it is essential to quantify the processes and controls on wetland C dynamics, including CH<sub>4</sub> emission, for assessing the impacts of climate change or management alternatives on wetland ecosystems.

<sup>1</sup>Now at Environmental Monitoring Section, Canada Center for Remote Sensing, Ottawa, Ontario, Canada.

[3] Carbon cycles and CH<sub>4</sub> emission in wetland ecosystems are regulated by a series of interacting processes between soil, hydrology, and vegetation. For example, hydrological processes have a great impact on soil thermal dynamics; soil thermal and hydrological conditions influence both plant growth and soil C dynamics (e.g., decomposition, CH<sub>4</sub> production, and oxidation); plant growth affects hydrological processes through evapotranspiration and intercepting precipitation; and soil, water, and plants work in conjunction to affect CH<sub>4</sub> production and transport. For handling these complex interactions, process-oriented models should be the most productive approach to synthesize our knowledge. There are few existing wetland models which are comprehensive enough to integrate most of the important processes for wetland ecosystems [Mitsch *et al.*, 1988] although many C models have been developed for upland ecosystems and used for global-scale C fluxes without explicitly identifying wetland ecosystems [Heimann *et al.*, 1998]. Trettin *et al.* [2001] evaluated 12 popular soil C models and found that they did not adequately account for anoxia, alternating hydroperiods, complex interactions of soil chemistry and abiotic factors, and CH<sub>4</sub> processes that are important to wetland C cycling.

[4] Existing wetland-related models generally fall into three categories: long-term peat accumulation models, empirical CH<sub>4</sub> emission models, and process-based CH<sub>4</sub> emission models. The peat accumulation models developed by Clymo [1984], Frohking *et al.* [2001], and others have been reviewed by Yu *et al.* [2001]. Frohking *et al.* [2001] developed a peat decomposition model (PDM) to calculate long-term peat accumulation based on vegetation conditions (NPP and rooting) and decomposition dynamics. This type of model focuses on long-term (several centuries to several millennia) peatland development and peat accumulation, and the effects of water table, vegetation, and climate are parameterized based on their average conditions, usually for specific sites. Empirical CH<sub>4</sub> emission models have been developed by directly correlating the observed CH<sub>4</sub> fluxes to controlling factors, such as water table, soil temperature, plant primary productivity, or ecosystem productivity [e.g., Bellisario *et al.*, 1999; Frohking and Crill, 1994; Moore and Roulet, 1993; Whiting and Chanton, 1993; Crill *et al.*, 1988]. These empirical relationships cannot be extrapolated to other sites where conditions are different from the experimental sites. Process-based models simulate CH<sub>4</sub> emissions with different degrees of complexity and integration with other processes [Cao *et al.*, 1996; Christensen *et al.*, 1996; Potter, 1997; Arah and Stephen, 1998; Grant, 1998; Walter and Heimann, 2000; Li, 2000]. Christensen *et al.* [1996] estimated CH<sub>4</sub> emissions as a constant ratio of soil heterotrophic respiration under steady state conditions. Potter [1997] simulated CH<sub>4</sub> production (CH<sub>4</sub>/CO<sub>2</sub> ratio) and CH<sub>4</sub> oxidation (fraction of CH<sub>4</sub>) as functions of water table depth. Walter and Heimann [2000] and Arah and Stephen [1998] predicted CH<sub>4</sub> production and oxidation based on Michaelis-Menten kinetics and simulated CH<sub>4</sub> transportation in soil and via plants. Their maximum CH<sub>4</sub> production and oxidation rates were parameterized without integration with vegetation and soil decomposition processes, and the models need water table

as input. Cao *et al.* [1996] considered the effects of environmental factors and substrates and the integrated processes of water table level, soil, and vegetation C dynamics in their simulation of CH<sub>4</sub> production and oxidation, although they used the Terrestrial Ecosystem Model (TEM) [Raich *et al.*, 1991] developed for upland ecosystems to handle the vegetation and soil C dynamics in their wetland studies. Grant [1998] simulated CH<sub>4</sub> emissions based on stoichiometries and energetics of the transformations mediated by each microbial community. His model may be the most complex CH<sub>4</sub> emission model, but was developed mainly for agricultural ecosystems. Li [2000] modified the DNDC model with detailed algorithms for simulating soil redox potential, substrate concentrations and CH<sub>4</sub> production, consumption and transport but only for rice paddies. We have adopted several of the above-listed approaches in the development of Wetland-DNDC, a more comprehensive wetland model.

[5] The purpose of developing Wetland-DNDC is to predict both CO<sub>2</sub> and CH<sub>4</sub> emissions driven by hydrology, soil biogeochemistry, and vegetation processes in wetland ecosystems. The model can run from a year to several decades with a primary time step of 1 day. This temporal scale allows us to directly use field observations to validate the model, and to answer questions about climatic change and management practices. The general structure of the model was adopted from PnET-N-DNDC, a process-oriented model simulating C and N dynamic and trace gas emissions in upland forest ecosystems [Li *et al.*, 2000]. PnET-N-DNDC was developed based on a basic biogeochemical concept, biogeochemical fields, which integrates the ecological drivers, environmental factors and geochemical and biochemical reactions into a dynamic system [Li *et al.*, 2000]. In comparison with the other 11 published biogeochemical models, PnET-N-DNDC provides a better framework for our development of a wetland C model [Trettin *et al.*, 2001]. For example, the ecological level and degree of complexity simulated by PnET-N-DNDC is a good match to the kinetic approaches adopted by Walter and Heimann [2000] and Cao *et al.* [1995, 1996] for modeling CH<sub>4</sub> fluxes from wetlands. In this paper, our discussion focuses on the new features developed in Wetland-DNDC, although Wetland-DNDC has inherited many existing functions from the DNDC model family (e.g., Crop-DNDC and PnET-N-DNDC). The distinguishing features of Wetland-DNDC include simulations of water table dynamics, effects of soil properties and hydrologic conditions on soil temperature, C fixation by mosses and herbaceous plants, and effects of anaerobic conditions on decomposition, CH<sub>4</sub> production and consumption, and other biogeochemical processes. Details of the model are described in section 2, followed by validation and sensitivity analysis in section 3.

## 2. Model Description

[6] Wetland-DNDC consists of four components: hydrological conditions, soil temperature, plant growth, and soil C dynamics (Figure 1). These four components and their processes interact closely with each other. For example, soil thermal and hydrological conditions influence plant growth

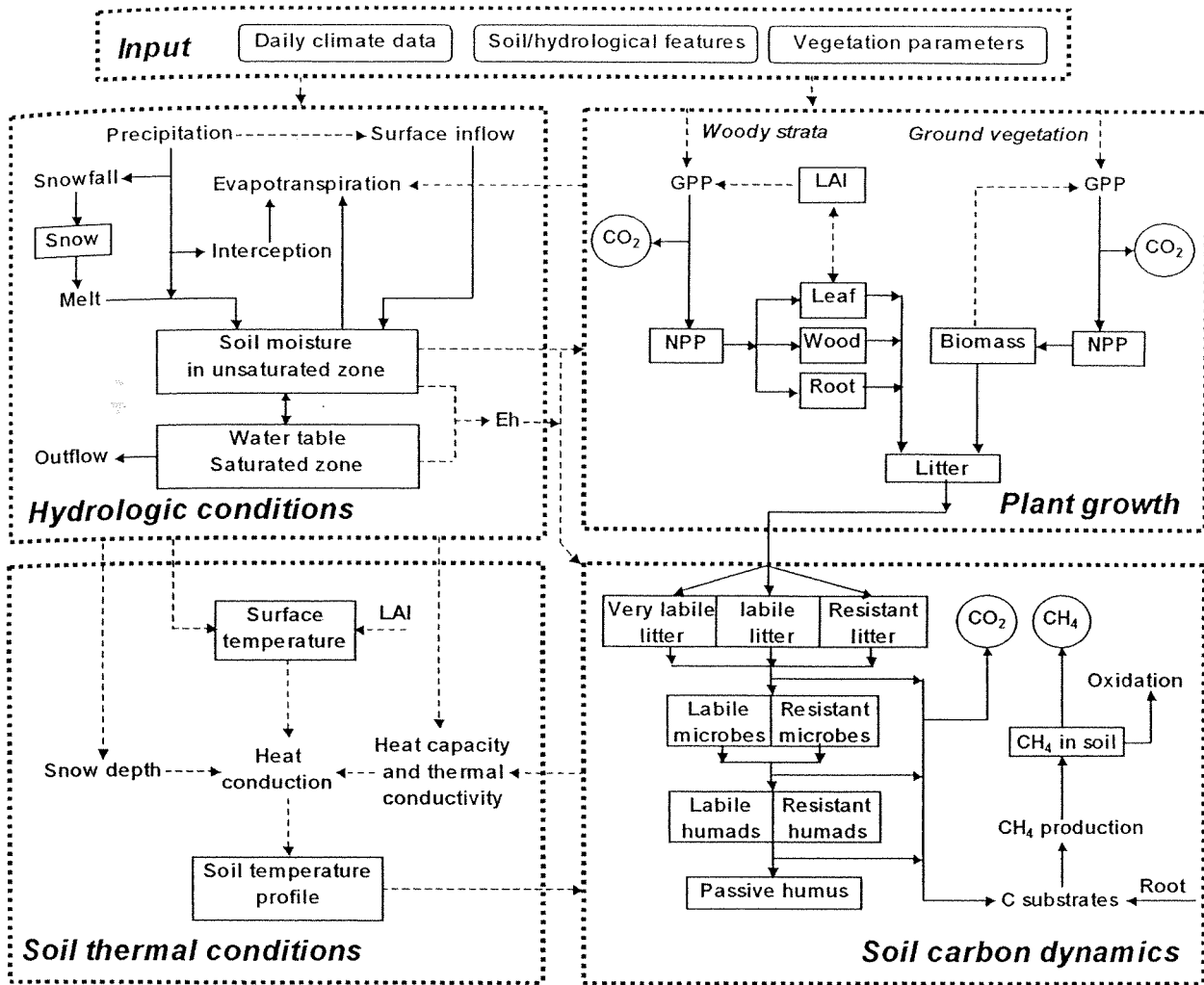


**Figure 1.** The conceptual structure of Wetland-DNDC. The model has four interacting components: hydrologic and thermal conditions, plant growth, and soil carbon dynamics. Solid lines are for matter flows, and dashed lines are for information flows. Rectangles are for major state variables, and circles are for gas emissions.

and soil C dynamics (e.g., decomposition,  $\text{CH}_4$  production, and oxidation). Plant growth influences evapotranspiration and precipitation interception and, thus, hydrological processes. Plant growth also affects  $\text{CH}_4$  emissions by providing C substrates for  $\text{CH}_4$  production and by providing conduits for  $\text{CH}_4$  transport. Wetland-DNDC explicitly considers all these processes and their interactions (Figure 1). The state variables are expressed as mass per unit area or relative content, representing a spatially homogeneous area or site as defined by the input data. The model input includes initial conditions (e.g., plant biomass, soil porosity, soil C content, water table position), model parameters (e.g., lateral inflow/outflow parameters, maximum photosynthesis rate, respiration rate), and climate drivers (e.g., daily maximum and minimum temperature, precipitation, solar radiation). The model output includes C pools and fluxes (e.g., C in plants and soil, photosynthesis, plant respiration, soil decomposition,  $\text{CH}_4$  emissions, and net ecosystem productivity), and thermal/hydrological conditions (e.g., soil mois-

ture, water table position, water fluxes, soil temperature profile). Soil C pools and their decomposition processes are described in detail in DNDC [Li *et al.*, 1992], and the dynamics of woody stratum are described in PnET [Aber *et al.*, 1996; Aber and Federer, 1992]. Below we describe the major improvements and the new developments of Wetland-DNDC in (1) hydrology, (2) soil thermal dynamics, (3) growth of mosses and herbaceous plants, and (4) anaerobic processes (decomposition,  $\text{CH}_4$  emissions).

## 2.1. Hydrology

[7] The hydrological submodel was developed to simulate water table dynamics explicitly. The soil profile is divided into layers of different characteristics (e.g., organic soils and mineral soils). The soil layers are then grouped into two zones: the unsaturated zone above the water table and the saturated zone below it. The hydrological submodel considers water table dynamics, aboveground water input (e.g., precipitation, surface inflow, snow/ice melt) and output

(evaporation, transpiration), and water movement in the unsaturated zone.

### 2.1.1. Soil Moisture and Water Table Dynamics

[8] The soil moisture content is determined for the unsaturated and the saturated zones separately. In the unsaturated zone, the soil moisture is determined by

$$\Delta SW_l H_l = F_l - ES_l - TP_l \quad (1)$$

where  $\Delta SW_l$  is the change of soil moisture ( $\text{cm}^3 \cdot \text{cm}^{-3}$ ) in layer  $l$  in the unsaturated zone,  $H_l$  is the thickness (cm) of the layer,  $F_l$  is net water input to the layer (cm water) through infiltration, gravity drainage, and matric redistribution, and  $ES_l$  and  $TP_l$  are water uptake (cm) from this layer through evaporation and transpiration, respectively. In the top saturated layer where water table resides (i.e., layer  $l_0$ ), the soil moisture is estimated by

$$SW_{l_0} = FC_{l_0} + (PS_{l_0} - FC_{l_0})WT'/H_{l_0} \quad (2)$$

where  $SW_{l_0}$  is the soil moisture ( $\text{cm}^3 \cdot \text{cm}^{-3}$ ) of layer  $l_0$ ,  $PS_{l_0}$  is the porosity ( $\text{cm}^3 \cdot \text{cm}^{-3}$ ),  $FC_{l_0}$  is the field capacity ( $\text{cm}^3 \cdot \text{cm}^{-3}$ ),  $WT'$  is the water table position in layer  $l_0$  (cm above the bottom of layer  $l_0$ ), and  $H_{l_0}$  is the thickness (cm) of the layer.

[9] Water table dynamics are determined directly by the water budget of the saturated zone, which includes water input from the unsaturated zone through infiltration and gravity drainage, capillary uptake through matric redistribution, evaporation and transpiration uptake from this zone, and outflow. The water budget is given by

$$\Delta WT \text{ Yield} = F_{l_0} - \sum_{l=l_0}^n (ES_l + TP_l) - \text{Outflow} \quad (3)$$

where  $\Delta WT$  is the change of water table position (cm),  $F_{l_0}$  is net water input (cm water) to the saturated zone from the above layers, and  $n$  is the total number of soil layers in the saturated zone.  $ES_l$  and  $TP_l$  are the same as those in equation (1). Yield ( $\text{cm}^3 \cdot \text{cm}^{-3}$ ) and outflow (cm water) are defined as

$$\text{Yield} = \begin{cases} PS_{l_0} - SW_{l_0} & \Delta WT \geq 0 \\ PS_{l_0} - FC_{l_0} & \Delta WT < 0 \end{cases} \quad (4)$$

$$\text{Outflow} = \begin{cases} a_1(WT - D_1) + a_2(WT - D_2) & WT > D_1 \\ a_2(WT - D_2) & D_2 < WT \leq D_1 \\ 0 & WT \leq D_2 \end{cases} \quad (5)$$

where  $SW_{l_0}$ ,  $PS_{l_0}$ , and  $FC_{l_0}$  are the same as those in equation (2), and  $WT$  is the water table position (cm) in reference to the soil surface.  $WT$  is positive when the water table is above the soil surface, and negative otherwise.  $\Delta WT > 0$  means that  $WT$  becomes higher.  $a_1$ ,  $a_2$ ,  $D_1$ , and  $D_2$  are calibrated parameters for outflows.  $D_1$  and  $D_2$  represent two critical levels (cm) of  $WT$ . Outflow increases linearly when  $WT$  is higher than these levels.  $a_1$  and  $a_2$  are the rates of increase. Because  $D_1$  is usually close to the surface and  $D_2$  is deeper along the soil profile,  $a_1(WT - D_1)$  and  $a_2(WT - D_2)$  are regarded as surface outflow and ground outflow, respectively.

### 2.1.2. Aboveground Water Input and Output

[10] Aboveground water input includes precipitation, snow/ice melt, and surface inflow. We followed the work of *Running and Coughlan* [1988] to determine plant interception of precipitation and snowmelt

$$P_{\text{int}} = \min(P, 0.05 \text{ LAI}) \quad (6)$$

$$W_{\text{melt}} = \min(\text{SNOW}, 0.07 T_m) \quad T_m > 0 \quad (7)$$

where  $P_{\text{int}}$  is the daily plant interception (cm),  $P$  is the daily precipitation (cm), and  $\text{LAI}$  is the leaf area index.  $W_{\text{melt}}$  is the amount of snow or ice melted in 1 day (cm in water),  $\text{SNOW}$  is the snowpack accumulated above the surface (cm in water), and  $T_m$  is the daily mean air temperature ( $^{\circ}\text{C}$ ). For depressional wetlands and most peatlands, surface lateral inflow usually comes from surface runoff of the watershed [*Mitsch and Gosselink*, 1993], and can be expressed as

$$S_{\text{in}} = (r - 1)R_p P \quad (8)$$

where  $S_{\text{in}}$  is the daily surface inflow (cm) expressed as water depth in the wetland,  $r$  is the ratio of the area of the watershed to the area of the wetland, and  $R_p$  is a hydrologic response coefficient.  $R_p$  represents the fraction of precipitation in the watershed that contributes directly to surface runoff. In the model, we combined  $(r - 1)R_p$  as one parameter ( $\alpha_0$ ).

[11] Both the potential evapotranspiration rate and water availability are considered in simulating evaporation and transpiration. We used the Priestley-Taylor approach [*Priestley and Taylor*, 1972; *Ritchie et al.*, 1988] to estimate potential evapotranspiration because it requires only daily solar radiation and temperature as input climate data. Potential evapotranspiration ( $ET_p$ ) is separated into potential soil evaporation ( $ES_p$ ) and potential plant transpiration ( $TP_p$ ) [*Ritchie et al.*, 1988]

$$ES_p = \begin{cases} ET_p(1 - 0.40 \text{ LAI}) & \text{LAI} < 1 \\ ET_p \exp(-0.43 \text{ LAI}) & \text{LAI} \geq 1 \end{cases} \quad (9)$$

$$TP_p = ET_p - ES_p \quad (10)$$

where  $ES_p$  and  $TP_p$  are in units of  $\text{cm} \cdot \text{day}^{-1}$ . Evapotranspiration will first consume water intercepted by plants or water on the soil surface, and then water from the soil profile. The actual water uptake from a soil layer for transpiration is determined by the potential demand and the root uptake rate

$$TP_l = R_{\text{max}} \text{RLD}_l f_{ET,l} H_l \quad (11)$$

where  $TP_l$  is the water uptake rate from layer  $l$  (cm water-day $^{-1}$ ),  $R_{\text{max}}$  is the maximum water uptake rate of a unit root length density from a cubic centimeter soil (cm water-day $^{-1} \cdot \text{cm}^{-1}$  root-cm $^{-3}$  soil),  $\text{RLD}_l$  is the root length density in layer  $l$  (cm root-cm $^{-3}$  soil),  $H_l$  is the thickness (cm) of layer  $l$ , and  $f_{ET,l}$  is a scalar.  $\text{RLD}_l$  is converted from root bio-mass using a specific root length of 2.1 cm-mg $^{-1}$  [*Eissenstat and Rees*, 1994].  $f_{ET,l}$  ranges from 0 to 1, representing the effects of soil moisture on evaporation and transpiration

$$f_{ET,l} = \begin{cases} 0 & T_l < 0 \text{ or } SW_l < WP_l \\ (SW_l - WP_l)/(FC_l - WP_l) & WP_l \leq SW_l < FC_l \\ 1 & SW_l \geq FC_l \end{cases} \quad (12)$$

where  $WP_l$  is the soil moisture ( $\text{cm}^3 \cdot \text{cm}^{-3}$ ) of layer  $l$  at the wilting point,  $FC_l$  is the field capacity ( $\text{cm}^3 \cdot \text{cm}^{-3}$ ), and  $T_l$  is the soil temperature of layer  $l$ .

### 2.1.3. Water Movement in the Unsaturated Zone

[12] The hydrological submodel considers three types of water movement in the unsaturated zone: infiltration, gravity drainage, and matric redistribution. Daily infiltration is a function of the infiltration capacity and the amount of water available on the soil surface. If water available for infiltration is more than the infiltration capacity, the excessive water will stay on the surface as ponds. The infiltration capacity depends further on water table position, saturated conductivity, and the frozen layer depth. If no frozen layer exists and the water table is low, the infiltration capacity is estimated as the amount of water infiltrated in a period of 24 h. Otherwise, the infiltration capacity is the amount of water saturating all the layers above the frozen layer or above the water table level. Gravity drainage refers to the downward movement of water when soil moisture is higher than field capacity. In our model, we assume that a fraction of water above field capacity will move to the next layer each day. Matric redistribution refers to the water movement driven by the gradient of matric potential between layers. The movement can be upward or downward. Matric redistribution is estimated based on the soil moisture difference of the two adjacent layers [Ritchie et al., 1988]. This procedure can include the capillary uptake of water from water table.

## 2.2. Soil Thermal Dynamics

[13] The soil temperature submodel estimates the daily average temperature of each soil layer by numerically solving the one-dimensional (vertical) heat conduction equation

$$C \frac{\partial T}{\partial t} = \frac{\partial}{\partial Z} \left( \lambda \frac{\partial T}{\partial Z} \right) \quad (13)$$

where  $C$  is the heat capacity ( $\text{J} \cdot \text{cm}^{-3} \cdot ^\circ\text{C}^{-1}$ ),  $T$  is the soil temperature ( $^\circ\text{C}$ ),  $t$  is time (s),  $\lambda$  is the thermal conductivity ( $\text{W} \cdot \text{cm}^{-1} \cdot ^\circ\text{C}^{-1}$ ), and  $Z$  is the soil depth (cm). The effects of soil water conditions and organic matter content on temperature can be expressed as their effects on  $C$  and  $\lambda$

$$C = \sum_{i=1}^5 f_i C_i \quad (14)$$

$$\lambda = \sum_{i=1}^5 f_i \lambda_i \quad (15)$$

where  $f_i$  is the fraction (volumetric ratio) of a given soil component  $i$  (i.e., minerals, water, ice, organic matter, and air), and  $C_i$  and  $\lambda_i$  are the heat capacity and the thermal conductivity of component  $i$ , respectively.

[14] The temperature of the top and the bottom soil layers defines the boundary conditions needed to solve equation (13). The top layer can be snowpack (when a snowpack exists), or water (when there is no snowpack and the water table is above the surface), or soil (when a snowpack does not exist and the water table is below the surface). The

temperature of the top layer is estimated based on the daily air temperature [Zheng et al., 1993]

$$T_0 = \begin{cases} T'_0 + 0.25(T_m - T'_0) \exp(-KLA) & T_m \geq T'_0 \\ T'_0 + 0.25(T_m - T'_0) & T_m < T'_0 \end{cases} \quad (16)$$

where  $T_0$  and  $T'_0$  are the temperatures of the top layer on the current day and the previous day, respectively,  $T_m$  is the air temperature on the current day, LAI is the leaf area index, and  $K$  is the light extinction coefficient. When a snowpack exists, mosses and herbaceous plants beneath the snowpack can effectively insulate heat conduction. Such insulation effects are considered by assuming a 5 cm moss/herbaceous layer with bulk density of  $33.3 \text{ (kg m}^{-3}\text{)}$  and water content of  $0.4 \text{ (g water} \cdot \text{g}^{-1} \text{ biomass)}$  [Frolking et al., 1996]. The depth of the snowpack is estimated based on snow accumulation (snowfall and snowmelt) and snow density. We assume that precipitation will be in the form of snow when daily air temperature ( $T_m$ ) is below  $0^\circ\text{C}$ . Snowpack is considered as one layer. Snow density increases each day by  $0.001T_m$  when  $T_m$  is higher than  $0^\circ\text{C}$ , based on an approximation of a detailed hourly snow model [Kongoli and Bland, 2000]. Snow density is set to  $0.1 \text{ g} \cdot \text{cm}^{-3}$  for fresh snow, and limited to  $0.3 \text{ g} \cdot \text{cm}^{-3}$  as the upper value [Verseghy, 1991]. Snowmelt is a function of temperature [Running and Coughlan, 1988] (equation (7)). Thermal conductivity and heat capacity of snow are estimated based on snow density [Mellor, 1977].

[15] The bottom boundary temperature is estimated by

$$T_{z_0} = T_{aa} + \exp(-Z_0/D) T_{am} \cos[2\pi(\text{JD} - \text{JD}_0)/365 - Z_0/D] \quad (17)$$

where  $T_{z_0}$  is the soil temperature of the bottom layer with a depth of  $Z_0$  (cm) on day JD,  $T_{aa}$  and  $T_{am}$  are the annual average and amplitude of air temperature, respectively, JD is the Julian date, and  $\text{JD}_0$  is the Julian day when solar altitude is the highest (i.e., 200th and 20th for the Northern and the Southern hemispheres, respectively).  $D$  is the damping depth (cm), given by

$$D = [365 \times 864 \lambda_m / (\pi C_m)]^{0.5} \quad (18)$$

where  $C_m$  is the average heat capacity of the soil profile ( $\text{J} \cdot \text{cm}^{-3} \cdot ^\circ\text{C}^{-1}$ ), and  $\lambda_m$  is the average thermal conductivity ( $\text{W} \cdot \text{cm}^{-1} \cdot ^\circ\text{C}^{-1}$ ) of the soil profile.

## 2.3. Growth of Mosses and Herbaceous Plants

[16] Mosses and herbaceous plants (hereafter, ground vegetation) are much more important for C fixation in wetlands compared to upland forest ecosystems. Therefore, we added algorithms for C fixation by ground vegetation to the vegetation submodel. Photosynthesis is estimated similarly to the moss simulation model of SPAM [Frolking et al., 1996]

$$\text{GPP}_g = A_{\text{max},g} B_g f_{g,L} f_{g,T} f_{g,WDL} \quad (19)$$

where  $\text{GPP}_g$  is the daily gross photosynthesis of ground vegetation ( $\text{kg C} \cdot \text{ha}^{-1} \cdot \text{day}^{-1}$ ),  $A_{\text{max},g}$  is the maximum photosynthesis rate per unit of effective photosynthetic biomass per hour ( $\text{kg C} \cdot \text{kg}^{-1} \text{ C} \cdot \text{h}^{-1}$ ),  $B_g$  is the effective

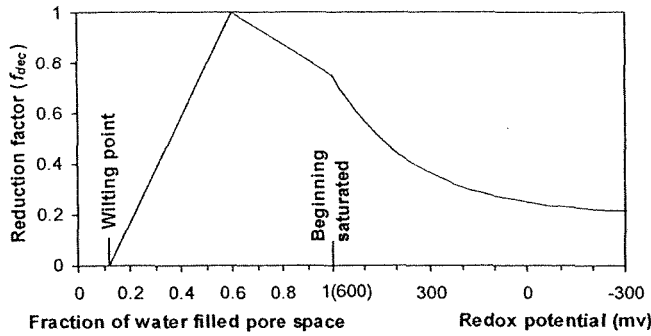


**Figure 2.** The effects of soil moisture (under unsaturated conditions) and redox potential (under saturated conditions) on soil organic carbon decomposition.

photosynthetic biomass of ground vegetation ( $\text{kg C}\cdot\text{ha}^{-1}$ ), DL is the day-length ( $\text{hr}\cdot\text{day}^{-1}$ ), and  $f_{g,L}$ ,  $f_{g,T}$ , and  $f_{g,W}$  are scalars that quantify the effects of light, temperature, and soil moisture, respectively.  $B_g$  is a function of the maximum aboveground biomass and the growing degree-days of the site;  $B_g$  represents changes in the amount of photosynthetically active tissues and the photosynthesis capacity of ground vegetation with time or phenology [Skre and Oechel, 1981; Williams and Flanagan, 1998]. We assume that the total daily respiration of plants is proportional to the daily  $GPP_g$ . Annual litter fall of ground vegetation is estimated as its annual net primary productivity (NPP) [Frolking et al., 1996]. The growth of woody strata is simulated based on PnET [Aber et al., 1996; Aber and Federer, 1992].

## 2.4. Anaerobic Processes

[17] In wetland ecosystems, soil C pools and fluxes and decomposition processes are strongly controlled by anaerobic conditions and, thus, hydrology. Anaerobic processes, such as  $\text{CH}_4$  production and oxidation, are unique features of wet soils and are critical to our understanding and prediction of C dynamics in wetlands. To deal with soil anaerobic conditions, existing models use water table either to define the boundary between the anoxic and the oxic zones [Walter and Heiman, 2000], or to modify  $\text{CH}_4$  production and oxidation rates [Cao et al., 1996; Potter, 1997]. However, after the soil has been inundated, soil anaerobic status changes with time, and  $\text{CH}_4$  production has a time delay of about 1–2 weeks [Patrick and Reddy, 1977]. In contrast, redox potential is a direct indicator of soil anaerobic status, and is closely related to the soil biochemical reactions [Mitsch and Gosselink, 1993; Fiedler and Sommer, 2000]. In Wetland-DNDC, we used the redox potential of the soil layers in the saturated zone to simulate the anaerobic effects on decomposition and  $\text{CH}_4$  production and oxidation.

### 2.4.1. Redox Potential and SOC Decomposition

[18] Redox potential ( $Eh$ ) is used to quantify the relative degree of anaerobic status for the soil layers near and below water table.  $Eh$  is estimated based on its general variation patterns in soils with a fluctuating water table [Sigren et al., 1997] and in soils under continuously

submerged conditions [Patrick and Reddy, 1977; Fiedler and Sommer, 2000]

$$\Delta Eh_l = \begin{cases} CR(A_l - 1) & l < l_0 \\ CR(A_l + 1 - wfps_l) & l \geq l_0 \end{cases} \quad (20)$$

where  $\Delta Eh_l$  is the daily variation of redox potential of layer  $l$  ( $\text{mv}\cdot\text{day}^{-1}$ ), CR is the rate of change (i.e.,  $100 \text{ mv}\cdot\text{day}^{-1}$ ),  $A_l$  is the aerenchyma factor of the layer, and  $wfps_l$  is the fraction of water filled pore space when the water table is below the top of this layer.  $A_l$  defines the plant-mediated gas transport (i.e., equivalent to the fraction of pore space for gas diffusion).

$$A_l = FRD P_A RLD_l \quad (21)$$

where FRD is the area of the cross section of a typical fine root ( $\text{cm}^2$ ),  $P_A$  is a scalar for the degree of gas diffusion from root to the atmosphere, and  $RLD_l$  is the root length density ( $\text{cm root}\cdot\text{cm}^{-3}$  soil) in layer  $l$ . FRD is assumed to be a constant of  $0.0013 \text{ cm}^2$  [Barber and Silberbush, 1984].  $P_A$  ranges from 0 (plants without aerenchyma) to 1 (plants with well developed aerenchyma). Grasses and sedges are good gas transporters ( $P_A = 1$ ), whereas trees are poor ones ( $P_A = 0.5$ ). Mosses are not considered for this effect because they are not vascular plants ( $P_A = 0$ ).

[19] Decomposition is slow under anaerobic conditions. The reported ratios of anaerobic decomposition to aerobic decomposition are 1:1.5–1:3 [Bridgham and Richardson, 1992], 1:2–1:4 [Chamie and Richardson, 1978], 1:3 [DeBusk and Reddy, 1998], 1:5 [Clymo, 1965], and 1:2.5–1:6 [Moore and Dalva, 1997]. Based on these results, we used the following relationship to estimate the effects of anaerobic status on decomposition for soil layers below the water table

$$f_{dec} = 0.2 + 0.05 \exp(Eh/250) \quad (22)$$

where  $f_{dec}$  is a scalar for the anaerobic effects on decomposition. For the soil layers above water table, soil moisture is used to estimate  $f_{dec}$  [Li et al., 1992]. Figure 2 shows the change of  $f_{dec}$  with changes of soil moisture and redox potential.

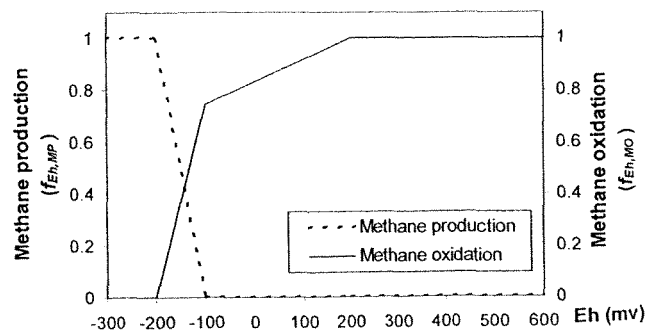


**Figure 3.** Effects of redox potential ( $Eh$ ) on methane production ( $f_{Eh, MP}$ ) and oxidation ( $f_{Eh, OX}$ ). The relationships are generalized from the study of Fiedler and Sommer [2000], Segers [1998], and Mitsch and Gosselink [1993].

**Table 1.** The Initial Conditions, Model Parameters, and Data Sources at SSA-Fen

Parameters	Values	References
<i>Lateral Water Flow</i>		
Surface inflow ( $\alpha_0$ )	0.2	calibrated <sup>a</sup>
Surface outflow ( $\alpha_1, D_1$ )	0.0, 0	calibrated <sup>a</sup>
Ground outflow ( $\alpha_2, D_2$ )	0.0002, -50	calibrated <sup>a</sup>
<i>Ground Vegetation</i>		
Biomass, kg C·ha <sup>-1</sup>	1950	<i>Suyker et al.</i> [1997]
$A_{\max, g}$ , g C·kg <sup>-1</sup> C·ha <sup>-1</sup>	3.73	<i>Suyker et al.</i> [1997]
Respiration (fraction of daily GPP)	0.5	calibrated <sup>a</sup>
Half saturation light, $\mu\text{mol}\cdot\text{m}^{-2}\cdot\text{s}^{-1}$	40	<i>Frolking et al.</i> [1996]
Minimum, optimum and maximum GDD (°C·d)	500, 1200, 2300	calibrated <sup>a</sup>
Soil pH	7.1	<i>Suyker et al.</i> [1996]

<sup>a</sup>Lateral water flow parameters were calibrated by comparing the simulated and measured water table. Plant respiration parameter was determined by comparing the simulated and the measured annual NPP. Minimum, optimum and maximum growing degree days (GDD) were determined based on the phenology of the plant growth (beginning, maximum, and senescence) and climate data.

#### 2.4.2. Methane Production, Oxidation, and Emissions

[20] To simulate CH<sub>4</sub> production, oxidation, and transport in Wetland-DNDC, we linked a process-based CH<sub>4</sub> emission model [Walter and Heiman, 2000] directly to soil thermal and hydrological conditions, soil redox potential, decomposition, and vegetation dynamics. Following the study by Walter and Heiman [2000], the change of CH<sub>4</sub> content in each layer ( $\Delta M$ ) is given by

$$\Delta M = M_{\text{PRD}} - M_{\text{OXD}} - M_{\text{DFS}} - M_{\text{EBL}} - M_{\text{PLT}} \quad (23)$$

where  $M_{\text{PRD}}$  and  $M_{\text{OXD}}$  are the CH<sub>4</sub> production rate and the oxidation rate, respectively,  $M_{\text{DFS}}$  is the diffusion between layers or to the atmosphere, and  $M_{\text{EBL}}$  and  $M_{\text{PLT}}$  are the CH<sub>4</sub> emissions through ebullition and plant-mediated transport from the layer, respectively. All these terms are in unit of kg C·ha<sup>-1</sup>·day<sup>-1</sup>.

[21] Methane production occurs in all soil layers if there are enough substrates and if environmental conditions are favorable [Fiedler and Sommer, 2000]. We simulated CH<sub>4</sub> production from each layer, using an approach similar to the ones used by Cao *et al.* [1995, 1996] and Walter and Heiman [2000], but with explicit consideration of the effects of redox potential

$$M_{\text{PRD}} = C_M f_{\text{T,MP}} f_{\text{pH}} f_{\text{Eh,MP}} \quad (24)$$

where  $C_M$  is the amount of simple C substrates (from soil decomposition and root systems) available for CH<sub>4</sub> production, and  $f_{\text{pH}}$ ,  $f_{\text{T,MP}}$ ,  $f_{\text{Eh,MP}}$  are scalars for the effects of temperature, pH, and redox potential on CH<sub>4</sub> production, respectively. The C substrate from roots is estimated as 45% of the C transferred to roots from photosynthesis [Cao *et al.*, 1995]. We calculated the pH effect based on the study of Cao *et al.* [1995], but used a minimum pH of 4.0 (instead of 5.5) because CH<sub>4</sub> emissions have been observed when pH is below 5.5 in wetlands [Crill *et al.*, 1988; Valentine *et al.*, 1994]. Walter and Heiman [2000] use a  $Q_{10}$  value of 6 to represent the effects of temperature on CH<sub>4</sub> production. We used a  $Q_{10}$  value of 3 because the temperature effects on  $C_M$  for methanogenesis have already been included in the calculation for soil organic carbon decomposition [Li *et al.*, 1992]. Methanogenesis requires a very low redox potential. Based on measurements and the literature review by Fiedler

and Sommer [2000], we used -200 and -100 mv as the two critical Eh values that define the effects of redox potential on CH<sub>4</sub> production (Figure 3).

[22] Methane oxidation is primarily controlled by the CH<sub>4</sub> concentration, redox potential, and temperature [Segers, 1998]. Methane oxidized in a soil layer is estimated by

$$M_{\text{OXD}} = M f_M f_{\text{T,MO}} f_{\text{Eh,MO}} \quad (25)$$

where  $M$  is the amount of CH<sub>4</sub> in a soil layer (kg C·ha<sup>-1</sup>), and  $f_M$ ,  $f_{\text{T,MO}}$ , and  $f_{\text{Eh,MO}}$  are scalars, representing the effects of CH<sub>4</sub> concentration, temperature, and redox potential, respectively. Based on the work of Walter and Heiman [2000], the effects of CH<sub>4</sub> concentration are expressed as

$$f_M = M_C / (K_m + M_C) \quad (26)$$

where  $M_C$  is the CH<sub>4</sub> concentration in a layer ( $\mu\text{mol}\cdot\text{L}^{-1}$ ), and  $K_m$  is a constant (e.g.,  $5 \mu\text{mol}\cdot\text{L}^{-1}$ ) [Walter and Heiman, 2000]. A  $Q_{10}$  value of 2 is chosen to quantify the effects of soil temperature on the oxidation rate [Segers, 1998]. We consider the effects of redox potential on CH<sub>4</sub> oxidation (Figure 3) based on the general patterns of CH<sub>4</sub> oxidation rates and soil redox potentials [Segers, 1998; Fiedler and Sommer, 2000; Mitsch and Gosselink, 1993].

[23] The CH<sub>4</sub> diffusion process is estimated with empirical relationships. In a daily time step, the CH<sub>4</sub> concentration gradient between two adjacent layers in the saturated zone decreases by about 70%, and is fully mixed in air filled space. Actual diffusion rates between layers and from the top layer to the atmosphere were estimated based on soil water content.

[24] Methane in each layer can be directly emitted to the atmosphere through ebullition and plant-mediated emission [Walter and Heiman, 2000]. Ebullition emission is considered when the soil CH<sub>4</sub> concentration in a layer exceeded a threshold concentration of  $750 \mu\text{mol}\cdot\text{L}^{-1}$  [Walter and Heiman, 2000]. The plant-mediated emission is estimated based on the plant aerenchyma factor (i.e.,  $A_i$  defined in equation (21))

$$M_{\text{PLT}} = MA_i(1 - P_{\text{OX}}) \quad (27)$$

where  $M_{\text{PLT}}$  is plant-mediated emission from a soil layer ( $l$ ), and  $P_{\text{OX}}$  is the fraction of CH<sub>4</sub> oxidized during the

**Table 2.** The Initial Conditions, Model Parameters, and Data Sources at MEF-Bog

Parameters	Values	References
<i>Lateral Water Flow</i>		
Surface inflow ( $\alpha_0$ )	0.5	calibrated <sup>a</sup>
Surface outflow ( $\alpha_1, D_1$ )	0.05, 0	calibrated <sup>a</sup>
Ground outflow ( $\alpha_2, D_2$ )	0.0005, -150	calibrated <sup>a</sup>
<i>Ground Vegetation</i>		
Biomass, kg C·ha <sup>-1</sup>	1750	Grigal [1985]
$A_{max,g}$ , g C·kg <sup>-1</sup> C·h <sup>-1</sup>	1.57	Skre and Oechel [1981]
Respiration (fraction of daily GPP)	0.2	calibrated <sup>a</sup>
Half saturation light, $\mu\text{mol}\cdot\text{m}^{-2}\cdot\text{s}^{-1}$	40	Frolking et al. [1996]
Minimum, optimum and maximum GDD, °C·d	100, 1300, 2500	calibrated <sup>a</sup>
Soil pH	3.9	Dise [1991]
<i>Woody Stratum</i>		
Summer time LAI	1.74	Grigal et al. [1985]
Aboveground woody biomass, kg C·ha <sup>-1</sup>	50365	Grigal et al. [1985]
Specific leaf area weight, g·m <sup>-2</sup> leaf	180.7	Gower et al. [1997]
Root, kg C·ha <sup>-1</sup>	71.3	Grigal et al. [1985] and Gower et al. [1997]
Foliage N concentration, %	0.88	Gower et al. [1997]
$A_{max,w}$ , nmol CO <sub>2</sub> ·g <sup>-1</sup> ·s <sup>-1</sup>	24.2	Aber et al. [1996]
Half saturation light, $\mu\text{mol}\cdot\text{m}^{-2}\cdot\text{s}^{-1}$	200	Aber et al. [1996]
Foliage retention time, yrs	11	Gower et al. [1997]
Begin and end foliage flushing GDD, °C·d	400, 1000	based on phenology and climate data
Begin senescence (Julian date)	230	based on phenology and climate data

<sup>a</sup> See the note in Table 1.

plant-mediated transport (i.e., 0.5) [Walter and Heimann, 2000].

### 3. Model Testing

[25] We tested Wetland-DNDC against field observations, including water table dynamics, soil temperature, CH<sub>4</sub> emissions, NEP, and annual C budget. A sensitivity analysis was also performed to determine critical parameters.

#### 3.1. Sites and Data

[26] We selected three northern wetland sites where extensive measurements are available: one in Saskatchewan, Canada, and two in Minnesota, USA. The first wetland site is a minerotrophic fen located about 115 km northeast of Alberta, Saskatchewan, Canada (53°57'N, 105°57'W). This site (referred hereafter as SSA-Fen) is in the southern study area of the Boreal Ecosystem-Atmosphere Study (BOREAS) [Sellers et al., 1997]. Suyker et al. [1996, 1997] give detailed descriptions of the site. Fluxes of CO<sub>2</sub> and CH<sub>4</sub> were measured in the growing seasons (from mid May to early October) of 1994 and 1995 by the eddy covariance technique, together with measurements of water table positions, plant species composition, and LAI [Suyker et al., 1996, 1997]. All the data were obtained from the BOREAS CD-ROM [Newcomer et al., 1999]. The second wetland site is a forested bog located in the Marcell Experimental Forest in Itasca County, Minnesota, USA (47°32'N, 93°28'W). This site (referred hereafter as MEF-Bog) is managed by the USDA Forest Service North Central Research Station. Dise [1991] and Verry and Urban [1992] give detailed descriptions of the site. Dise [1991] measured CH<sub>4</sub> emissions at MEF-Bog from 1989 to 1990

using open-bottom chambers, together with soil temperature and water table positions. In addition, the daily water table dynamics have been monitored since 1961 [Verry and Urban, 1991]. The third wetland site is a bog lake peatland located about 2 km from the MEF-Bog site. This site (referred hereafter as BLP-Fen) is characterized as a poor fen with carpet-forming mosses (*Sphagnum papillosum*) dominating the vegetation. Detailed descriptions of the site can be found in the study by Shurpali et al. [1993, 1995] and Kim and Verma [1992]. Both CO<sub>2</sub> and CH<sub>4</sub> fluxes were measured in 1991 and 1992 by the eddy covariance technique [Shurpali et al., 1993, 1995].

#### 3.2. Initial Conditions and Model Parameters

[27] The initial conditions and parameter values used in the model testing are given in Table 1 (SSA-Fen), Table 2 (MEF-Bog), and Table 3 (BLP-Fen). First, we identified the difference in vegetation covers at the three sites. For SSA-Fen, the ground vegetation alone was used to determine the overall plant C fixation (Table 1) because of low tree density [Suyker et al., 1997]. For MEF-Bog, both woody

**Table 3.** The Initial Conditions, Model Parameters, and Data Sources at BLP-Fen

Parameters	Values	References
<i>Lateral Water Flow</i>		
Surface inflow ( $\alpha_0$ )	1.0	calibrated <sup>a</sup>
Surface outflow ( $\alpha_1, D_1$ )	0.1, 10	calibrated <sup>a</sup>
Ground outflow ( $\alpha_2, D_2$ )	0.006, -50	calibrated <sup>a</sup>
Ground vegetation: parameters and their values are the same as those at MEF-Bog in Table 2		
Soil pH	4.6	Kim and Verma [1992]

<sup>a</sup> See the note in Table 1.



**Table 4.** The Soil Characteristics Along Soil Profiles Used in Simulations at the Three Study Sites<sup>a</sup>

Depth, cm	Bulk Density	Porosity	Field Capacity	Wilting Point
5	0.09	0.94	0.51	0.12
75	0.13	0.91	0.64	0.16
200	0.24	0.84	0.69	0.22

<sup>a</sup> The data are based on the works of Zoltai *et al.* [2000] and Paavilainen and Päivänen [1995]. All of the four soil characteristics are in the unit of  $\text{cm}^3 \cdot \text{cm}^{-3}$ .

plants and ground vegetation were simulated explicitly (Table 2). For BLP-Fen, the same ground vegetation as for MEF-Bog was used, but woody plants were absent at this site (Table 3). Second, the active soil profile at the three sites was assumed to be 2 m in-depth and composed of peat. The distributions of bulk density, field capacity, and wilting point are given in Table 4, on the basis of the study by Zoltai *et al.* [2000] and Paavilainen and Paivanen [1995]. Third, the parameters of lateral water flow were determined by comparing the simulated and the measured water table (i.e., using the first 3 years' measurements at MEF-Bog and the 2 years' measurements at the other sites). Fourth, the micro-topographic effects (i.e., hollows and hummocks) on the overall C fluxes measured by the eddy covariance technique can be assessed based on the relative height of the peat surface [Clement *et al.*, 1995]. At MEF-Bog, the data for the microsites of hollows and hummocks were reported separately; thus, we ran the model for each micro site directly using the measured water table as input. At SSA-Fen and BLP-Fen, however, the micro-topographic effects were not reported. To better reflect these effects on C flux predictions, we obtained the average water table for

the average hollow site, ran the model with this average water table and with four different surface heights above the hollow surface (i.e., 0, 10, 20, and 30 cm), calculated the average C fluxes from these four runs, and used the average C fluxes to compare with the tower measured C fluxes.

[28] Sensitivity analysis was conducted with the data from BLP-Fen in 1992 (Tables 3 and 4) as the baseline conditions. The model parameters, initial conditions, and climate drivers were changed one at a time to determine their effects on model predictions. The response variables used in the sensitivity analysis are water table, NPP, soil microbial respiration,  $\text{CH}_4$  emissions, and NEP.

### 3.3. Results and Discussions

#### 3.3.1. Hydrology

[29] The long-term measurements of water table dynamics from 1961 to 1999 at MEF-Bog provide an excellent data set for model validation. The model predictions correspond well to the trends and the temporal variations of the water table measurements (Figure 4;  $R^2 = 0.54$ ,  $N = 14244$ ); most of the unexplained variance may be a result of mismatches in the exact timing and exact values of water table change. The model also captured the variation patterns of surface outflow (Figure 5;  $R^2 = 0.52$ ,  $N = 468$ ), but the simulated surface outflow was about 46% higher than the measured stream outflow, perhaps due to water loss from places other than the measuring station at the stream outlet. The model estimates a ground outflow of 2–2.7  $\text{cm} \cdot \text{month}^{-1}$  (aside from a low value of 1.3  $\text{cm} \cdot \text{month}^{-1}$  in 1977). Although there was no direct measurement of ground outflow, a slow, steady seepage must have existed because the water table was perched several meters above the regional water table [Verry and Urban, 1992]. The

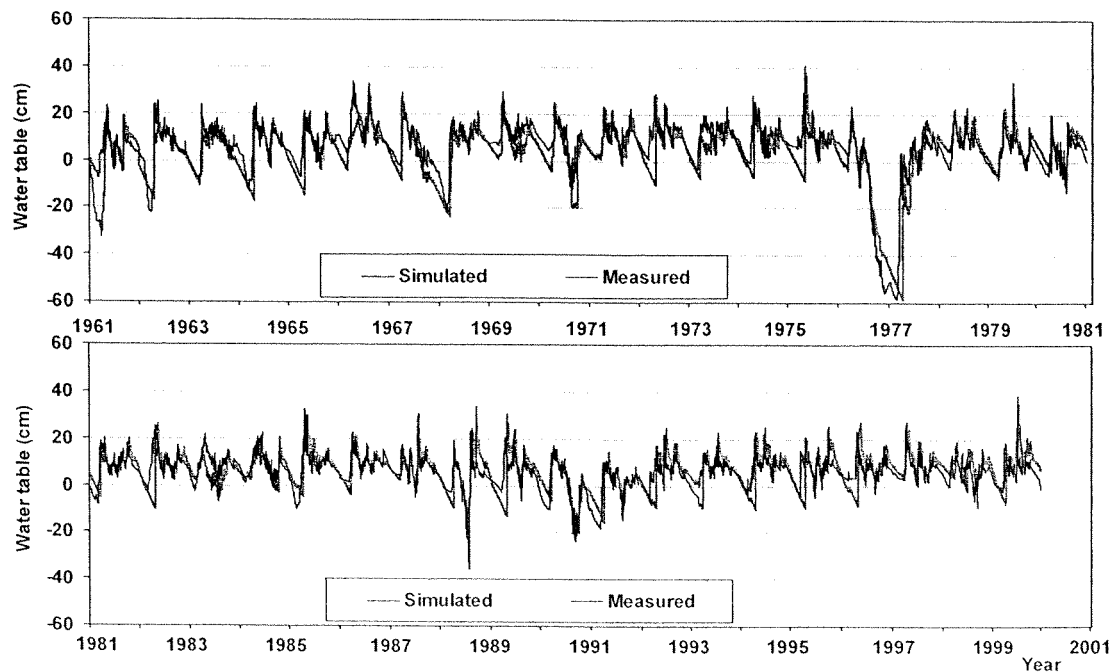


**Figure 4.** Comparisons between simulated and measured water table dynamics at MEF-Bog in Minnesota, USA.

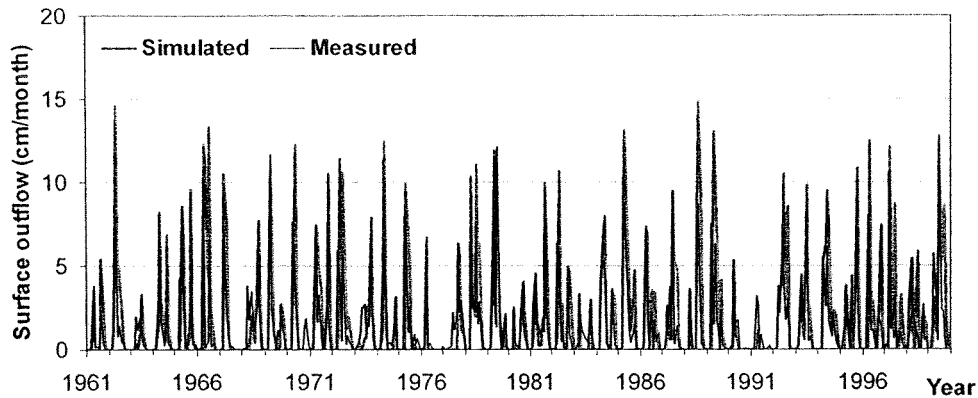


Figure 5. Comparisons between simulated and measured surface outflow at MEF-Bog in Minnesota, USA. The measurements were conducted at a stream outlet.

model also works well in predicting evapotranspiration ( $R^2 = 0.62$ ,  $N = 263$ . Years 1994 and 1996) and snowpack ( $R^2 = 0.83$ ,  $N = 1021$ . Years 1994–1996) at SSA-Fen where measurements were available. These results indicate that the hydrologic model can quantify water table dynamics and water fluxes of wetlands at the watershed scale.

### 3.3.2. Soil Temperature

[30] Figure 6 shows comparisons between simulated and measured soil temperature at different depths of the hollow site at MEF-Bog. The model accurately predicts the trajectories of the measured soil temperature along the soil profile, with  $R^2$  values ranging from 0.88 to 0.91 (with sample sizes of 45–59). Similar results are also obtained for the hummock site at MEF-Bog and for SSA-Fen (results not shown here). The model captures the effects of snow and soil organic matter on soil temperature. For example, due to the insulating effects of the moss layer and snowpack, soil temperature stays near or above  $0^\circ\text{C}$  in winter and spring although air temperature could be as low as  $-30^\circ\text{C}$  during this period. Soil temperature in deeper layers (e.g., 40 cm) may be  $4^\circ\text{C}$  lower than in the top layer in summer, but about  $1^\circ\text{C}$  higher than in the top layers in winter.

### 3.3.3. Methane Emissions

[31] The  $\text{CH}_4$  emission model was tested at all three sites. The model captures general patterns of  $\text{CH}_4$  emissions, including the annual total, inter-annual differences, and the effects of water table positions (Figure 7). Values of  $R^2$  ranged from 0.37 to 0.76 with sample sizes of 47–214, except at MEF-Bog hummock, where  $R^2 = 0.03$  ( $N = 42$ ), because  $\text{CH}_4$  emission is very low. At SSA-Fen,  $\text{CH}_4$  emissions are largely correlated with plant growth and soil decomposition because the water table is almost always above the surface. The simulated annual  $\text{CH}_4$  emissions ( $\text{kg C}\cdot\text{ha}^{-1}\cdot\text{yr}^{-1}$ ) are 122.1 for 1994 and 121.0 for 1995 (Figure 7A). The estimated  $\text{CH}_4$  emissions from the tower flux measurements were  $163 \text{ kg C}\cdot\text{ha}^{-1}$  for the period from May 17 of 1994 to October 7 of 1994 [Suyker et al., 1996]. The difference between simulated and observed  $\text{CH}_4$  emissions in 1994 may be caused by an underestimation of peak  $\text{CH}_4$  emissions and late growing season emissions. Although the water table was above the hollow surface, it fluctuated in a wider range in 1994 than in 1995. In 1994, the water table

increased from 5 cm in late May to 26 cm in late July, then declined to 3 cm in late September. In 1995, the water table declined from 25 cm in late May to 14 cm in late September. In general, the model overestimates  $\text{CH}_4$  emissions when water table increases, but underestimates  $\text{CH}_4$  emissions when water table decreases. We suspect that these simulation errors may be caused by: (1) combination effects of micro-topography and water table fluctuation, (2) trapping and releasing of  $\text{CH}_4$  during water table fluctuations, and (3) effects of water layer thickness since the model assumes that the water table will have the same effects on anaerobic conditions and  $\text{CH}_4$  transport when water table is above the surface, regardless of depth.

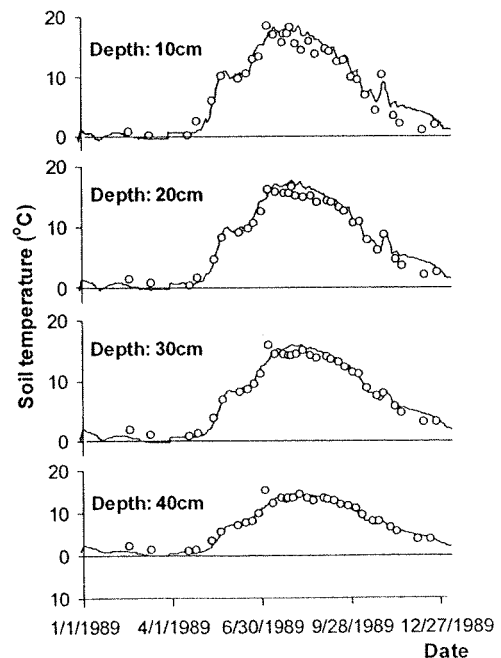
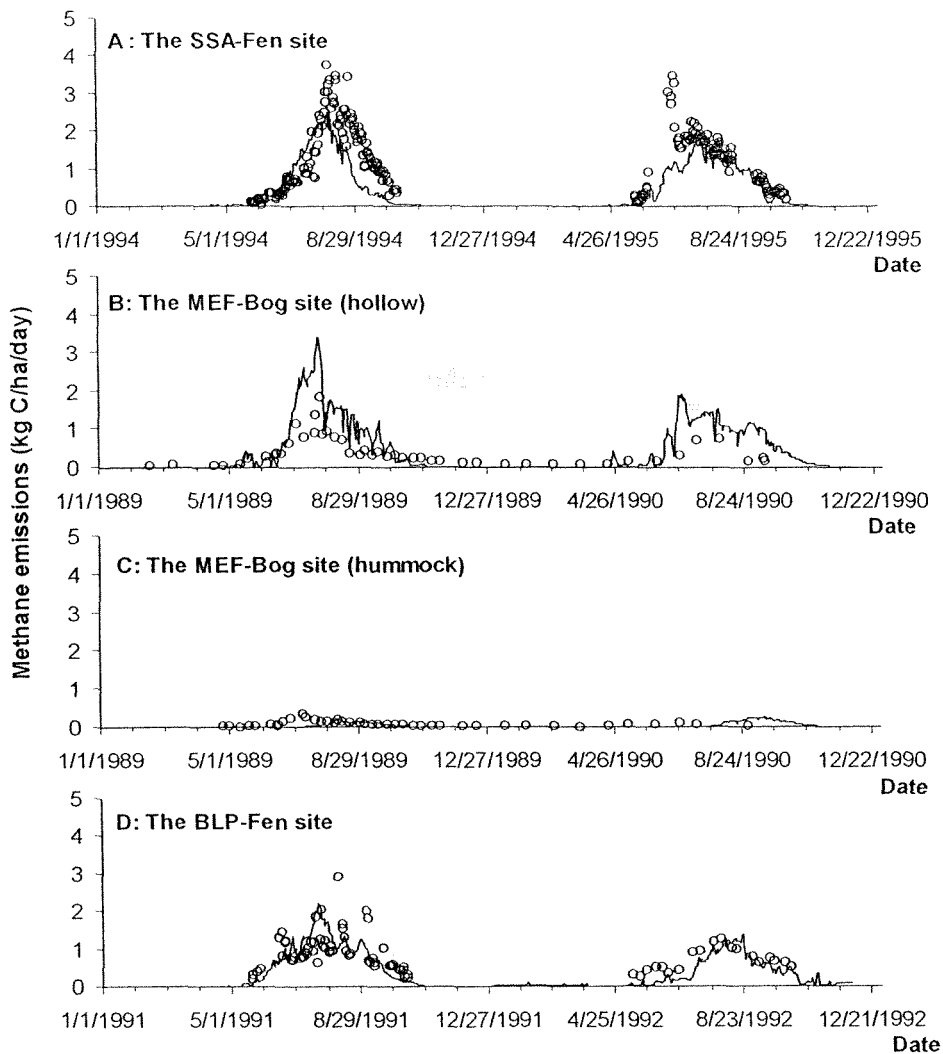


Figure 6. Comparisons between simulated (curves) and measured (circles) soil temperature along a soil profile at MEF-Bog in Minnesota, USA. The data are for the hollow site measured by *Dise* [1991].



**Figure 7.** Comparisons between simulated (curves) and measured (circles) methane emissions at the three study sites: SSA-Fen in Saskatchewan, Canada, MEF-Bog (hollow versus hummock) in Minnesota, USA, and BLP-Fen in Minnesota, USA. The measurements at BLP-Fen in 1991 are daytime totals from the work of *Shurpali et al.* [1993], while all other measurements and the simulated results are daily totals.

[32] At MEF-Bog,  $\text{CH}_4$  emissions from the hummock site are much smaller than those from the hollow site (Figure 7B, C) because the average water table for the hummocks is 38 cm below the surface compared to 7 cm below the surface for the hollows. The simulated annual  $\text{CH}_4$  emissions ( $\text{kg C}\cdot\text{ha}^{-1}\cdot\text{yr}^{-1}$ ) for the hollow site are 157.1 for 1989 and 127.0 for 1990, while they are 8.6 for 1989 and 14.0 for 1990 at the hummock site. The estimated  $\text{CH}_4$  emissions ( $\text{kg C}\cdot\text{ha}^{-1}$ ) from observations from April 1 of 1989 to March 31 of 1990 were 103.5 for the hollows and 26.3 for the hummocks [*Dise*, 1991].

[33] At BLP-Fen, the model predictions display good agreement with the observations (Figure 7D). Note that in Figure 7D, the  $\text{CH}_4$  measurements of 1991 are the daytime totals reported by *Shurpali et al.* [1993], whereas the measurements for 1992 are daily totals reported by *Clement et al.* [1995]. The simulated annual  $\text{CH}_4$  emissions are  $129.2 \text{ kg C}\cdot\text{ha}^{-1}\cdot\text{yr}^{-1}$  for 1991, which is within the range of the

observed values of  $120.0\text{--}146.3 \text{ kg C}\cdot\text{ha}^{-1}\cdot\text{yr}^{-1}$  reported for 1991 [*Shurpali et al.*, 1993]. The simulated annual  $\text{CH}_4$  emissions for 1992 are  $87.8 \text{ kg C}\cdot\text{ha}^{-1}\cdot\text{yr}^{-1}$ . The lower  $\text{CH}_4$  value in 1992 may be due to the relatively stable and high water table that limits soil decomposition and, therefore, reduces C substrates for  $\text{CH}_4$  production.

### 3.3.4. $\text{CO}_2$ Flux and C Budget

[34] Wetland-DNDC also predicts other C fluxes and the annual C budget in addition to  $\text{CH}_4$  emissions. Figure 8 shows the variation patterns of NEP, NPP, and soil decomposition (i.e., soil microbial  $\text{CO}_2$  emissions) at SSA-Fen and BLP-Fen. There were no observed daily fluxes of NPP and soil decomposition at these two sites. However, we present the simulated NPP and soil decomposition to aid in understanding the variation patterns of NEP and the annual C budget.

[35] At SSA-Fen, predicted NEP was compared to the measured daily NEP during the period of 1994–1995. The model captures the general pattern of NEP (Figure 8A) ( $R^2 =$

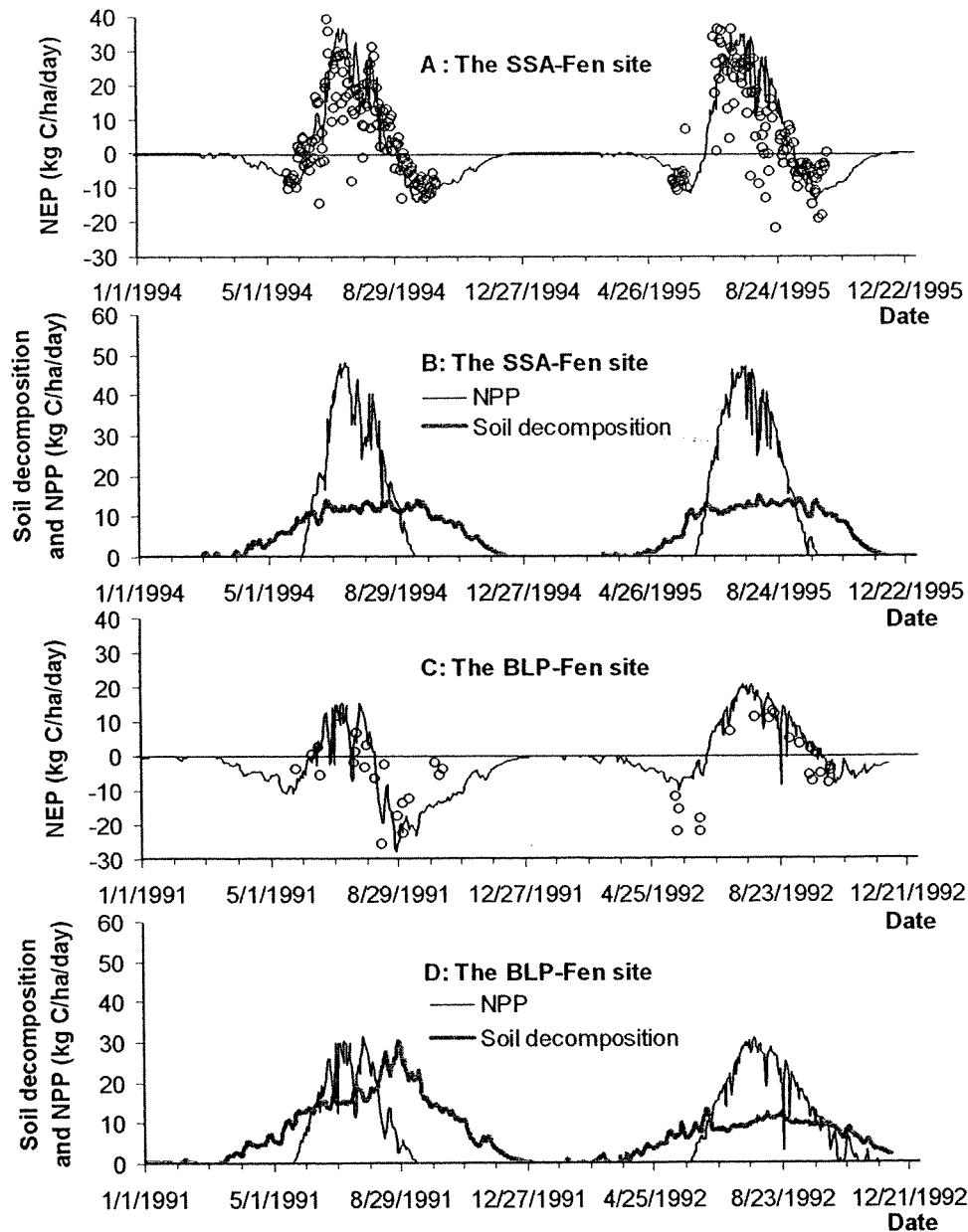


**Figure 8.** The dynamics of net ecosystem exchange (NEP), net primary productivity (NPP), and soil decomposition. (a) Comparisons between simulated NEP (curves) and measured NEP (circles) at SSA-Fen; (b) simulated NPP and soil decomposition at SSA-Fen; (c) comparisons between simulated NEP (curves) and measured NEP (circles) at BLP-Fen; and (d) simulated NPP and soil decomposition at BLP-Fen.

0.49,  $N = 266$ ). The simulated total NEP from mid-May to early October in 1994 is  $958.4 \text{ kg C}\cdot\text{ha}^{-1}$ , which agrees closely with the measured NEP of  $880 \text{ kg C}\cdot\text{ha}^{-1}$  for the same period [Suyker *et al.*, 1997]. NEP is a function of the combined effects of plant C fixation and soil C decomposition (Figure 8B). The simulated annual NPP ( $\text{kg C}\cdot\text{ha}^{-1}\cdot\text{yr}^{-1}$ ) is 2589.8 for 1994 and 2878.1 for 1995, while the field measured aboveground NPP in 1994 was  $1950 \text{ kg C}\cdot\text{ha}^{-1}\cdot\text{yr}^{-1}$  [Suyker *et al.*, 1996]. The simulated soil decomposition ( $\text{kg C}\cdot\text{ha}^{-1}\cdot\text{yr}^{-1}$ ) is 2128.3 for 1994 and 2023.9 for

1995. The annual C sequestration ( $\text{kg C}\cdot\text{ha}^{-1}\cdot\text{yr}^{-1}$ ), which included  $\text{CO}_2$  exchange and  $\text{CH}_4$  emissions, is calculated as 339.4 for 1994 and 733.2 for 1995. The average annual C sequestration for these 2 years is  $536.3 \text{ kg C}\cdot\text{ha}^{-1}\cdot\text{yr}^{-1}$ . This value is higher than the average long-term wetland C accumulation rate ( $210 \text{ kg C}\cdot\text{ha}^{-1}\cdot\text{yr}^{-1}$ ) estimated by Clymo *et al.* [1998], perhaps because this site is more productive than moss-dominated wetlands and because the high water table during these 2 years may have reduced soil decomposition.

Table 5. Simulated Annual Carbon Budget of the MEF-Fen Site<sup>a</sup>

Year		1989			1990		
		Woody Strata	Ground Vegetation	Total	Woody Strata	Ground Vegetation	Total
Hollow	GPP	7129.9	1986.5	9116.4	7538.8	2194.1	9732.9
	NPP	3647.8	1589.2	5237.0	3877.4	1755.3	5632.7
	plant growth	2318.7	0.0	2318.7	2496.7	0.0	2496.7
	litter production	1329.1	1589.2	2918.3	1380.7	1755.3	3136.0
	soil microbial respiration			1864.8			2495.8
	CH <sub>4</sub> emissions			157.1			127.0
	soil C balance			896.4			513.2
	C sequestration			3215.1			3009.9
Hummock	GPP	8589.7	1999.6	10589.3	7779.7	2196.5	9976.2
	NPP	3933.8	1599.7	5533.5	4026.2	1757.2	5783.4
	plant growth	2532.5	0.0	2532.5	2604.3	0.0	2604.3
	litter production	1401.3	1599.7	3001.0	1421.9	1757.2	3179.1
	soil microbial respiration			2954.3			3487.3
	CH <sub>4</sub> emissions			8.6			14.0
	soil C balance			38.1			-322.2
	C sequestration			2570.6			2282.1

<sup>a</sup>Unit: kg C ha<sup>-1</sup> yr<sup>-1</sup>.

[36] At BLP-Fen, the model also captures the general pattern of NEP, displaying good agreement between the predicted and the measured daily NEP during the period of 1991–1992 (Figure 8C) ( $R^2 = 0.59$ ,  $N = 40$ ). The simulated NEP (kg C·ha<sup>-1</sup>) for the period from mid May to mid October is -910.2 for 1991 and 931.0 for 1992, while the measured NEP for the same period was -710 for 1991 and 320 for 1992 [Shurpali et al., 1995]. The simulated NEP for early 1992 is much higher than the measurements largely because the model fails to capture the sizable C release during the pre-leaf period when C trapped in soils from decomposition in late fall and winter was released as soil thawed [Lafleur et al., 1997]. The simulated NPP of the ground vegetation shows a rapid decline and then an early termination in the fall of 1991 (Figure 8D) because of drought effects. During the period of May–October, total precipitation in 1991 was about 30% less than that in 1992, and the mean temperature in 1991 was 1.5°C higher than that in 1992. The simulated annual NPP (kg C·ha<sup>-1</sup>·yr<sup>-1</sup>) is 1754.2 for 1991 and 2436.9 for 1992. The simulated soil decomposition rate also reflects drought effects (i.e., high temperature, low precipitation, low water table) in 1991; the peak soil decomposition rate in 1991 was twice that in 1992 (Figure 8D). The simulated soil decomposition for the period from May to October of 1991 is 2939.3 kg C·ha<sup>-1</sup>, which is comparable to the measured value of 3654.5 kg C·ha<sup>-1</sup> (including root respiration) [Kim and Verma, 1992]. The simulated annual NEP (kg C·ha<sup>-1</sup>·yr<sup>-1</sup>) is -1581.8 for 1991 (source) and 470.7 for 1992 (sink). The annual C sequestration (kg C·ha<sup>-1</sup>·yr<sup>-1</sup>), including CO<sub>2</sub> exchange and CH<sub>4</sub> emissions, is -1711.0 for 1991 and 382.9 for 1992.

[37] There is no woody stratum at SSA-Fen and BLP-Fen. The annual change in soil C therefore is the same as NEP because we assume that the annual NPP of ground vegetation should be the same as its litter production. Table 5 shows the simulated annual C budget at MEF-Bog. Both the hollow and hummock sites are sinks of atmospheric CO<sub>2</sub> with the C accumulation occurring primarily in the woody strata. Although the mortality of the trees may greatly reduce this sequestration, as measured by Grigal et al.

[1985], the model currently does not consider mortality. Soil C increases at the hollow site, but changes little in 1998 and even decreases in 1990 at the hummock site. The average soil C balance of the hollow and hummock sites is 281.4 kg C·ha<sup>-1</sup>·yr<sup>-1</sup>, which is comparable to the 180–280 kg C·ha<sup>-1</sup>·yr<sup>-1</sup> estimated by Verry and Urban [1992]. They also found a soil C loss with water flow of 370 kg C·ha<sup>-1</sup>·yr<sup>-1</sup>. However, their estimate of soil microbial respiration (4710 kg C·ha<sup>-1</sup>·yr<sup>-1</sup>) was much higher than our simulated results. As a result, their estimate of litter input to soil would also be much higher, possibly due to tree mortality. The simulated NPP is 5434.9 and 5658.5 kg C·ha<sup>-1</sup>·yr<sup>-1</sup> at the hollow and hummock sites, respectively; these numbers are comparable to the above ground NPP of 3700 kg C·ha<sup>-1</sup>·yr<sup>-1</sup> measured by Grigal [1985] and Grigal et al. [1985].

### 3.3.5. Sensitivity Analysis

[38] Sensitivity analysis reveals the effects of given factors on selected state variables. The three groups of factors are initial conditions, model parameters, and climate drivers, while the five selected state variables are water table (WT), NPP, soil microbial respiration ( $R_s$ ), CH<sub>4</sub> emissions, and NEP. WT is given as absolute change, whereas the others are expressed as changes in percentage (Table 6).

[39] The five state variables respond differently to different input variables. WT and NPP are sensitive to only a few model parameters and environmental variables, whereas  $R_s$ , CH<sub>4</sub>, and NEP respond strongly to many (Table 6). One simple reason is that calculating C fluxes like CH<sub>4</sub> and NEP involves many components of Wetland-DNDC. WT is primarily influenced by hydrological parameters (e.g., the critical levels of outflow;  $D_1$  and  $D_2$  in (5)) and by climate variables (e.g., precipitation, temperature). A decrease in either  $D_1$  or  $D_2$  by 10 cm could lower the annual average WT by about 10 cm (Table 6); this is because outflow increases linearly with WT as soon as WT rises above these boundary levels. Such high sensitivity of WT to  $D_1$  and  $D_2$  indicates that good long-term WT data are essential since  $D_1$  and  $D_2$  (together with  $a_1$  and  $a_2$ ) are calibrated parameters (5). Furthermore, although an increase in precipitation

**Table 6.** Sensitivity Analysis of Wetland-DNDC<sup>a</sup>

Input Parameters and Variables	Change	$\Delta$ WT <sup>b</sup> , cm	$\Delta$ NPP, %	$\Delta$ R <sub>s</sub> , %	$\Delta$ CH <sub>4</sub> , %	$\Delta$ NEP, %
<i>Initial Conditions</i>						
Biomass	+10%	0.0	8.7	0.1	4.5	13.6
	-10%	0.0	-9.2	-0.1	-4.6	-14.6
Soil organic carbon	+10%	0.0	0.0	9.9	12.6	-12.5
	-10%	0.0	0.0	-9.9	-9.7	12.5
Soil pH	+0.5	0.0	0.0	0.0	18.3	0.0
	-0.5	0.0	0.0	0.0	-20.1	0.0
Porosity	+10%	0.0	-0.4	-5.0	-18.6	5.7
	-10%	-1.7	0.5	6.9	8.9	0.0
Field capacity	+10%	-1.3	0.0	-3.5	3.0	4.4
	-10%	0.0	0.0	-0.2	-3.6	0.2
<i>Parameters</i>						
Surface inflow ( $\alpha_0$ )	+10%	0.3	-0.1	-2.8	-3.7	3.5
	-10%	-1.5	0.2	0.7	-13.2	-0.6
Surface outflow rate ( $\alpha_1$ )	+10%	-0.1	0.0	-0.3	-4.3	-0.4
	-10%	0.2	0.0	0.1	0.9	0.1
Ground outflow rate ( $\alpha_2$ )	+10%	-2.5	0.2	-1.5	-14.1	2.2
	-10%	1.1	-0.1	-6.1	4.7	7.6
Critical level for surface outflow ( $D_1$ )	+10 cm	5.5	-0.1	-1.2	6.9	1.4
	-10 cm	-9.2	2.2	18.1	-51.4	-19.3
Critical level for ground outflow ( $D_2$ )	+10 cm	5.1	-0.1	-13.4	3.9	16.8
	-10 cm	-10.3	1.0	10.6	-28.8	-7.8
$A_{\max,g}$	+10%	0.0	9.0	0.0	4.7	14.4
	-10%	0.0	-9.3	0.0	-4.8	-14.9
Half saturation light	+10%	0.0	-0.9	0.0	-0.4	-1.5
	-10%	0.0	0.9	0.0	0.4	1.5
Respiration rate	+10%	0.0	-2.3	0.0	-1.2	-3.7
	-10%	0.0	2.3	0.0	1.2	3.7
Minimum GDD	+100°C·d	0.0	-3.8	0.0	-1.7	-6.0
	-100°C·d	0.0	-3.9	0.0	1.6	6.1
Optimal GDD	+100°C·d	0.0	-0.3	0.0	-0.6	-0.5
	-100°C·d	0.0	0.6	0.0	0.5	0.9
Maximum GDD	+100°C·d	0.0	1.9	0.0	0.5	3.0
	-100°C·d	0.0	2.4	0.0	-0.6	3.8
<i>Climate Drivers<sup>c</sup></i>						
Temperature	+2°C	-2.0	-12.4	63.5	10.5	-99.9
	-2°C	-2.1	-0.5	-35.6	-48.1	44.2
Precipitation	+10%	0.8	-0.1	-4.4	1.5	5.4
	-10%	-5.0	0.8	6.3	-20.9	-6.6
Solar radiation	+10%	-0.1	0.0	1.3	-0.4	0.0
	-10%	0.0	0.0	0.0	0.0	0.0

<sup>a</sup> The parameters are changed from the baseline data of BLP-Fen in Table 3, either by 10% or by a specified quantity. The selected response variables are the annual average water table ( $\Delta$ WT), net primary production ( $\Delta$ NPP), soil microbial respiration ( $\Delta$ R<sub>s</sub>), net ecosystem productivity ( $\Delta$ NEP), and methane emissions ( $\Delta$ CH<sub>4</sub>).

<sup>b</sup> Water table is expressed as the annual average, while the others are expressed as the annual totals.

<sup>c</sup> Changes of climate drivers are for each day based on daily climate data.

may produce limited effects on WT, a drought may exert greater influences on WT (Table 6). NPP is sensitive to the maximum photosynthesis rate ( $A_{\max,g}$  in equation (18)) and the initial biomass, similar to what was observed by *Aber et al.* [1996] for woody plants. In addition, while NPP shows little response to a decrease in temperature, it may be reduced by 12.4% with a 2°C temperature increase, perhaps because of increasing autotrophic respiration.  $R_s$  is significantly affected by temperature because temperature exerts direct effects on microbial activity and on soil moisture conditions. The simulations show that the number of days when WT is above the surface decreases dramatically from 171 days under the baseline condition to 85 days with a temperature increase of 2°C.  $R_s$  is also sensitive to changes in  $D_1$  and  $D_2$  and initial soil organic C. CH<sub>4</sub> responds strongly to temperature and  $D_1$  and  $D_2$ , and, to a lesser extent, to precipitation and initial soil conditions (e.g.,

organic C, pH, and porosity). For NEP, the most critical factors are temperature,  $D_1$  and  $D_2$ ,  $A_{\max,g}$ , plant biomass, and initial soil organic C.

[40] To further test the interactions between plant, soil, and hydrology, we conducted two simulation experiments. First, we arbitrarily controlled the C substrates for CH<sub>4</sub> production. Simulated annual CH<sub>4</sub> emissions decrease 49.4% when C substrates from plants are eliminated, while simulated CH<sub>4</sub> emissions decrease 69.6% when C substrates from soil decomposition are excluded. Second, we ran the model with constant water table levels (i.e., 20, 10, and 0 cm above the surface, and 10, 20, and 30 cm below the surface). When the water table is maintained at 10 cm above surface, annual CH<sub>4</sub> emissions are the highest, 89% of the baseline emissions. When water table is kept at 20 cm above surface, annual CH<sub>4</sub> emissions decrease by about 30% compared to that observed for a water table 10 cm above

the surface due to a decrease in soil decomposition and soil temperature. This suggests that a fluctuating water table may be more favorable for CH<sub>4</sub> emissions than a constant water table. Because the effect of water table on NPP is small, change in NEP is mostly due to the effect of water table on soil heterotrophic respiration. NEP is 1205.7 kg C·ha<sup>-1</sup>·yr<sup>-1</sup> with a water table 20 cm above the surface and -706.8 kg C·ha<sup>-1</sup>·yr<sup>-1</sup> with a water table 30 cm below the surface. The baseline NEP is 396.7 kg C·ha<sup>-1</sup>·yr<sup>-1</sup>. These results and the above sensitivity analysis show that C dynamics and CH<sub>4</sub> emissions respond differently to input factors and they also strongly depend on the interactions among thermal/hydrological conditions, plant growth, and soil C dynamics. It is therefore critical for models to integrate hydrology, vegetation, soil, and climate in predicting C exchange and CH<sub>4</sub> emissions of wetland ecosystems.

#### 4. Conclusions

[41] A biogeochemical model, Wetland-DNDC, was developed by integrating the complex processes of hydrology, soil biogeochemistry, and vegetation in wetland ecosystems. In comparison to its parent model (PnET-N-DNDC), Wetland-DNDC includes several important changes, which enable the new model to capture the specific features of wetland ecosystems. The major improvements include functions and algorithms for simulating water table dynamics, the effects of soil composition and hydrologic conditions on soil temperature, C fixation by mosses or other ground growth species, and the effects of anaerobic status on decomposition and CH<sub>4</sub> production/oxidation. Wetland-DNDC was tested against data sets of observed water table dynamics, soil temperature, CH<sub>4</sub> flux, CO<sub>2</sub> exchange, and annual C budget at three wetland sites in North America. The modeled results are in agreement with the observations. Sensitivity analysis indicates that wetland C dynamics are sensitive to temperature, water outflow rate, initial soil organic C content, plant photosynthesis capacity, and initial biomass in the wetland ecosystems. NEP and CH<sub>4</sub> fluxes are sensitive to a wide scope of input parameters of climate, soil, hydrology, and vegetation. The ecosystem C dynamics as well as the CH<sub>4</sub> emissions simulated by Wetland-DNDC respond to changes in thermal and hydrological conditions in a complex manner. The results further confirm the necessity of utilizing process models to integrate many interactions among climate, hydrology, soil, and vegetation for predicting C dynamics in wetland ecosystems.

[42] Wetland-DNDC currently does not include distribution hydrological routines to handle water inflow and outflow for a given watershed due to the complexity in calculation and amount of spatially differentiated input data required (e.g., topography, soil etc.). Instead, we focused this model at the site scale, and empirically parameterized the inflow and outflow indices for individual wetland watersheds where multiple-year observations of water table dynamics were available. For applying the model at large scales, these hydrological indices can be generated based on the normalized ranges or variations in water table and the lateral water fluxes. In this case, uncertainty analysis must be conducted to assess the

potential errors produced from the generalized hydrological parameters.

#### Notation

$A_l$	plant aerenchyma factor of layer $l$
$A_0$	plant specific aerenchyma factor, (cm <sup>2</sup> ).
$A_{\max,g}$	maximum photosynthesis rate of ground vegetation (kg C·kg C <sup>-1</sup> ·h <sup>-1</sup> ).
$A_{\max,w}$	maximum photosynthesis rate of woody plant (nmol CO <sub>2</sub> ·g <sup>-1</sup> ·s <sup>-1</sup> ).
$B_g$	efficient photosynthetic biomass of ground vegetation (kg C·ha <sup>-1</sup> ).
$C$	heat capacity of a layer (J·cm <sup>-3</sup> ·°C <sup>-1</sup> ).
$C_i$	heat capacity of component $i$ (J·cm <sup>-3</sup> ·°C <sup>-1</sup> ).
$C_M$	C substrate for CH <sub>4</sub> production in a soil layer (kg C·ha <sup>-1</sup> ).
CR	change rate of soil redox potential under saturated conditions (100 mv·day <sup>-1</sup> ).
$D$	damping depth (cm).
$D_1, D_2$	critical depths for lateral outflow (cm).
$D_l$	depth of soil layer $i$ (cm).
DL	day length (h·day <sup>-1</sup> ).
$Eh$	redox potential (mv).
$ES_l$	water lost through evaporation from layer $l$ (cm).
$ES_p$	potential soil evaporation (cm).
$ET_p$	potential evapotranspiration (cm).
$f_{dec}$	effects of redox potential and soil moisture on decomposition.
$f_i$	volumetric fraction of component $i$ in soil.
$f_{g,GDD}$	effects of growing degree days on amount of effective photosynthetic biomass.
$f_{gL}, f_{g,T}, f_{g,W}$	effects of light, temperature, and water on photosynthesis of ground vegetation, respectively.
$f_{ET,l}$	effects of soil moisture on evaporation and transpiration.
$f_{Eh,MP}$	effects of redox potential on CH <sub>4</sub> production.
$f_{Eh,MO}$	effects of redox potential on CH <sub>4</sub> oxidation.
$f_M$	effects of CH <sub>4</sub> concentration on CH <sub>4</sub> oxidation.
$F_{pH}$	effects of pH on CH <sub>4</sub> production.
$f_{T,MP}$	effects of temperature on CH <sub>4</sub> production.
$f_{T,MO}$	effects of temperature on CH <sub>4</sub> oxidation.
$FC_{l_0}$	field capacity of soil layer $l_0$ (cm <sup>3</sup> ·cm <sup>-3</sup> ).
$F_l, F_{l_0}$	net water input to layer $l$ and $l_0$ , respectively, through infiltration, gravity drainage, and matric redistribution (cm).
FRD	the area of the cross-section of a typical fine root (0.0013 cm <sup>2</sup> ).
$GPP_g$	gross photosynthesis of ground vegetation (kg C·ha <sup>-1</sup> ).
$H_l, H_{l_0}$	thickness of layer $l$ and $l_0$ , respectively (cm).
JD	Julian date.
$JD_0$	Julian date when solar altitude is the highest (200 for the Northern Hemisphere, 20 for the Southern Hemisphere).

$K_m$	a constant ( $5 \mu\text{mol}\cdot\text{L}^{-1}$ ) for effects of $\text{CH}_4$ concentration on $\text{CH}_4$ oxidation ( $\mu\text{mol}\cdot\text{L}^{-1}$ ).
$l_0$	soil layer in which water table resides.
LAI	leaf area index (one side area) ( $\text{m}^2\cdot\text{m}^{-2}$ ).
$M$	$\text{CH}_4$ content in a soil layer ( $\text{kg C}\cdot\text{ha}^{-1}$ ).
$M_c$	$\text{CH}_4$ concentration in a layer ( $\mu\text{mol}\cdot\text{L}^{-1}$ ).
$M_{\text{DIF}}$	$\text{CH}_4$ content decrease through diffusion ( $\text{kg C}\cdot\text{ha}^{-1}$ ).
$M_{\text{EBL}}$	$\text{CH}_4$ emission through ebullition ( $\text{kg C}\cdot\text{ha}^{-1}$ ).
$M_{\text{PLT}}$	$\text{CH}_4$ emission through plant-mediated transport ( $\text{kg C}\cdot\text{ha}^{-1}$ ).
$M_{\text{OXD}}$	$\text{CH}_4$ oxidation rate of a soil layer ( $\text{kg C}\cdot\text{ha}^{-1}$ ).
$M_{\text{PRD}}$	$\text{CH}_4$ production in a soil layer ( $\text{kg C}\cdot\text{ha}^{-1}$ ).
$N$	sample size.
$n$	number of layers above water table level.
Outflow	lateral outflow from the saturated zone (cm).
$P$	precipitation (cm).
$P_A$	relative capacity of a plant for gas diffusion from its root system to the atmosphere.
$P_{\text{int}}$	plant interception of precipitation (cm).
$P_{\text{ox}}$	fraction of $\text{CH}_4$ oxidized during plant mediated transport (0.5).
$\text{PS}_{l_0}$	porosity of soil layer $l_0$ ( $\text{cm}^3\cdot\text{cm}^{-3}$ ).
$R^2$	squared correlation coefficient.
$r$	ratio of the area of a watershed to the area of a wetland in the watershed.
$\text{RLD}_l$	root length density of layer $l$ ( $\text{cm}^{-2}$ ).
$R_{\text{max}}$	maximum root water uptake rate ( $0.003 \text{ cm}^2\cdot\text{day}^{-1}$ ).
$R_p$	the surface-runoff fraction of precipitation in a watershed.
$S_{\text{in}}$	surface inflow (cm).
SNOW	snowpack (cm water).
$\text{SW}_l, \text{SW}_{l_0}$	soil moisture of layer $l$ and $l_0$ , respectively ( $\text{cm}^3\cdot\text{cm}^{-3}$ ).
$t$	time (s).
$T, T_l$	soil temperature ( $^{\circ}\text{C}$ ).
$T_0, T'_0$	top surface temperature on the current day and the day before, respectively ( $^{\circ}\text{C}$ ).
$T_{\text{aa}}$	annual average air temperature ( $^{\circ}\text{C}$ ).
$T_{\text{am}}$	annual amplitude of air temperature ( $^{\circ}\text{C}$ ).
$T_{z_0}$	bottom layer soil temperature ( $^{\circ}\text{C}$ ).
$T_m$	daily mean air temperature ( $^{\circ}\text{C}$ ).
$\text{TP}_l$	water lost through transpiration from layer $l$ (cm).
$\text{TP}_p$	potential plant transpiration (cm).
$\text{wfps}_l$	fraction of water filled pore space.
$W_{\text{melt}}$	snowmelt (cm water).
$\text{WP}_l$	soil moisture at wilting point of layer $l$ ( $\text{cm}^3\cdot\text{cm}^{-3}$ ).
WT	water table position in reference to soil surface (cm).
$\text{WT}'$	height of water table level above the bottom of layer $l_0$ (cm).
Yield	amount of water required for a unit water table change ( $\text{cm cm}^{-1}$ ).
$Z$	depth (cm).
$Z_0$	depth of the bottom soil layer (cm).
$\alpha_0$	surface inflow relative to precipitation.

$\alpha_1, \alpha_2$	rate parameters for outflow.
$\lambda$	thermal conductivity of a layer ( $\text{W}\cdot\text{cm}^{-1}\cdot^{\circ}\text{C}^{-1}$ ).
$\lambda_i$	thermal conductivity of component $i$ ( $\text{W}\cdot\text{cm}^{-1}\cdot^{\circ}\text{C}^{-1}$ ).
$\Delta M$	change of $\text{CH}_4$ content in a soil layer ( $\text{kg C}\cdot\text{ha}^{-1}\cdot\text{day}^{-1}$ ).
$\Delta Eh$	change of redox potential ( $\text{mv}\cdot\text{day}^{-1}$ ).
$\Delta \text{SW}_l$	change of soil moisture in layer $l$ in the unsaturated zone ( $\text{cm}^3\cdot\text{cm}^{-3}\cdot\text{day}^{-1}$ ).
$\Delta \text{WT}$	change of water table position ( $\text{cm}\cdot\text{day}^{-1}$ ).

[43] **Acknowledgments.** The authors gratefully acknowledge the contributions of the source codes of PnET-N-DNDC provided by John Aber, Florian Stange, Klaus Butterback-Bahl, and Hans Papen. The authors are indebted to Nigel Roulet for supporting Yu Zhang to conduct his study in McGill University. The authors would like to thank the two anonymous reviewers for their comments and suggestions, and to Karen Bartlett for editing the paper. This study is funded by the USDA Forest Service Southern Global Change Program, U.S. multiagency TECO grant, NASA EOS-IDS grant, and the National Council on Air and Stream Improvement (NCASI).

## References

- Aber, J. D., and C. A. Federer, A generalized, lumped-parameter model of photosynthesis, evaporation and net primary production in temperate and boreal forest ecosystems, *Oecologia*, 92, 463–474, 1992.
- Aber, J. D., P. B. Reich, and M. L. Goulden, Extrapolating leaf  $\text{CO}_2$  exchange to the canopy: A generalized model of forest photosynthesis compared with measurements by eddy correlation, *Oecologia*, 10, 257–265, 1996.
- Arah, J. R. M., and K. D. Stephen, A model of the processes leading to methane emission from peatland, *Atmos. Environ.*, 32, 3257–3264, 1998.
- Aselmann, I., and P. J. Crutzen, Global distribution of natural freshwater wetlands and rice paddies, their net primary productivity, seasonality and possible methane emissions, *J. Atmos. Chem.*, 8, 307–358, 1989.
- Barber, S. A., and M. Silberbush, Plant root morphology and nutrient uptake, in *Roots, Nutrient and Water Influx, and Plant Growth, American Society of Agronomy*, edited by S. A. Barber and D. R. Bouldin, *Spec. Publ.* 49, pp. 65–87, Madison, WI, 1984.
- Bellisario, L. M., J. L. Bubier, T. R. Moore, and J. P. Chanton, Controls on  $\text{CH}_4$  emissions from a northern peatland, *Global Biogeochem. Cycles*, 13, 81–91, 1999.
- Bridgman, S. D., and C. J. Richardson, Mechanisms controlling soil respiration ( $\text{CO}_2$  and  $\text{CH}_4$ ) in southern peatlands, *Soil Biol. Biochem.*, 24, 1089–1099, 1992.
- Bubier, J. L., The relationship of vegetation to methane emission and hydrochemical gradients in northern peatlands, *J. Ecol.*, 83, 403–420, 1995.
- Bubier, J. L., P. M. Crill, T. R. Moore, K. Savage, and R. K. Varner, Seasonal patterns of controls on net ecosystem  $\text{CO}_2$  exchange in a boreal peatland complex, *Global Biogeochem. Cycles*, 12, 703–714, 1998.
- Cao, M., J. B. Dent, and O. W. Heal, Modeling methane emissions from rice paddies, *Global Biogeochem. Cycles*, 9, 183–195, 1995.
- Cao, M., S. Marshall, and K. Gregson, Global carbon exchange and methane emissions from natural wetlands: Application of a process-based model, *J. Geophys. Res.*, 101, 14,399–14,414, 1996.
- Chamie, J. P. M., and C. J. Richardson, Decomposition in northern wetlands, in *Freshwater Wetlands: Ecological Processes and Management Potential*, edited by R. E. Good, D. F. Whigham, and R. L. Simpson, pp. 115–130, Academic, San Diego, Calif., 1978.
- Christensen, T. R., I. C. Prentice, J. Kaplan, A. Haxeltine, and S. Sitch, Methane flux from northern wetlands and tundra: An ecosystem source modeling approach, *Tellus, Ser. B*, 48, 652–661, 1996.
- Clement, R. J., S. B. Verma, and E. S. Verry, Relating chamber measurements to eddy correlation measurements of methane flux, *J. Geophys. Res.*, 100, 21,047–21,056, 1995.
- Clymo, R. S., Experiments on breakdown of sphagnum in two bogs, *J. Ecol.*, 53, 747–758, 1965.
- Clymo, R. S., Limit of peat bog growth, *Philos. Trans. R. Soc. London, Ser. B*, 303, 605–654, 1984.
- Clymo, R. S., J. Turunen, and K. Tolonen, Carbon accumulation in peatland, *Oikos*, 81, 368–388, 1998.
- Crill, P. M., K. B. Bartlett, R. C. Harriss, E. Gorham, E. S. Verry, D. I. Sebacher, L. Madzar, and W. Sanner, Methane flux from Minnesota peatlands, *Global Biogeochem. Cycles*, 2, 371–384, 1988.



- DeBusk, W. F., and K. R. Reddy, Turnover of detrital organic carbon in a nutrient-impacted Everglades marsh, *Soil Sci. Soc. Am. J.*, *62*, 1460–1468, 1998.
- Dise, N. B., Methane emission from peatlands in Northern Minnesota, Ph.D. dissertation, p. 138, Univ. of Minnesota, Minneapolis, 1991.
- Eissenstat, D. M., and K. C. J. Van Rees, The growth and function of pine roots, *Ecol. Bull.*, *43*, 76–91, 1994.
- Eswaran, H., E. Van den Berg, P. Reich, and J. Kimble, Global soil carbon resources, in *Soils and Global Change*, edited by R. Lal et al., pp. 27–43, CRC Press, Boca Raton, Fla., 1995.
- Fiedler, S., and M. Sommer, Methane emissions, ground water levels and redox potentials of common wetland soils in a temperate-humid climate, *Global Biogeochem. Cycles*, *14*, 1081–1093, 2000.
- Frolking, S., and P. Crill, Climate controls on temporal variability of methane flux from a poor fen in southeastern New Hampshire: Measurement and modeling, *Global Biogeochem. Cycles*, *8*, 385–397, 1994.
- Frolking, S., et al., Modelling temporal variability in the carbon balance of a spruce/moss boreal forest, *Global Change Biol.*, *2*, 343–366, 1996.
- Frolking, S., N. T. Roulet, T. R. Moore, P. J. H. Richard, M. Lavoie, and S. D. Muller, Modeling northern peatland decomposition and peat accumulation, *Ecosystems*, *4*, 479–498, 2001.
- Gorham, E., Northern peatlands: Role in the carbon cycle and probable response to climate warming, *Ecol. Monogr.*, *1*, 182–195, 1991.
- Grant, R. F., Simulation of methanogenesis in the mathematical model ecosys, *Soil Biol. Biochem.*, *30*, 883–896, 1998.
- Grigal, D. F., *Sphagnum* production in forested bogs of northern Minnesota, *Can. J. Bot.*, *63*, 1204–1207, 1985.
- Grigal, D. F., C. G. Buttleman, and L. K. Kernik, Biomass and productivity of woody strata of forested bogs in northern Minnesota, *Can. J. Bot.*, *63*, 2416–2424, 1985.
- Heimann, M., et al., Evaluation of terrestrial carbon cycle models through simulations of the seasonal cycle of atmospheric CO<sub>2</sub>: First results of a model intercomparison study, *Global Biogeochem. Cycles*, *12*, 1–24, 1998.
- Kim, J., and S. B. Verma, Soil surface CO<sub>2</sub> flux in a Minnesota peatland, *Biogeochemistry*, *18*, 37–51, 1992.
- Kongoli, C. E., and W. L. Bland, Long-term snow depth simulation using a modified atmosphere-land model, *Agric. For. Meteorol.*, *104*, 273–287, 2000.
- Lafleur, P. M., J. H. McCaughey, D. W. Joiner, P. A. Bartlett, and D. E. Jelinski, Seasonal trends in energy, water, and carbon dioxide fluxes at a northern boreal wetland, *J. Geophys. Res.*, *102*, 29,009–29,020, 1997.
- Li, C., Modeling trace gas emissions from agricultural ecosystems, *Nutr. Cycling Agroecosyst.*, *58*, 259–276, 2000.
- Li, C., S. Frolking, and T. A. Frolking, A model of nitrous oxide evolution from soil driven by rainfall events, I, Model structure and sensitivity, *J. Geophys. Res.*, *97*, 9759–9776, 1992.
- Li, C., J. Aber, F. Stange, and H. Papen, A process-oriented model of N<sub>2</sub>O and NO emissions from forest soils, I, Model development, *J. Geophys. Res.*, *105*, 4369–4384, 2000.
- Matthews, E., and I. Fung, Methane emission from natural wetlands: Global distribution, area and environmental characteristics of sources, *Global Biogeochem. Cycles*, *1*, 61–86, 1987.
- Mellor, M., Engineering properties of snow, *J. Glaciol.*, *19*, 15–66, 1977.
- Mitsch, W. J., and J. G. Gosselink, *Wetlands*, 2nd ed., p. 722, Van Nostrand Reinhold, New York, 1993.
- Mitsch, W. J., M. Sraskraba, and S. E. Jorgensen (Eds.), *Wetland Modeling: Development in Environmental Modeling*, vol. 12, p. 227, Elsevier Science, New York, 1988.
- Moore, T. R., and M. Dalva, Methane and carbon dioxide exchange potentials of peat soils in aerobic and anaerobic laboratory incubations, *Soil Biol. Biochem.*, *29*, 1157–1164, 1997.
- Moore, T. R., and N. T. Roulet, Methane flux: Water table relations in northern wetlands, *Geophys. Res. Lett.*, *20*, 587–690, 1993.
- Newcomer, J., et al. (Eds.), *Collected Data of the Boreal Ecosystem-Atmosphere Study*, (CD-ROM), NASA, 1999.
- Paavilainen, E., and J. Päävönen, *Peatland Forestry, Ecology and Principles*, p. 248, Springer-Verlag, New York, 1995.
- Patrick, W. H., Jr., and C. N. Reddy, Chemical changes in rice soils, in *IRRI Symposium on Soils and Rice*, pp. 361–379, IRRI, Los Bano., Philippines, 1977.
- Potter, C. S., An ecosystem simulation model for methane production and emission from wetlands, *Global Biogeochem. Cycles*, *11*, 495–506, 1997.
- Priestly, C. H. B., and R. J. Taylor, On the assessment of surface heat flux and evaporation using large scale parameters, *Mon. Weather Rev.*, *100*, 81–92, 1972.
- Raich, J. W., E. B. Rastetter, J. M. Melillo, D. W. Kicklighter, P. A. Stender, B. J. Peterson, A. L. Grace, B. Moore III, and C. J. Vorosmarty, Potential net primary productivity in South America: An application of a global model, *Ecol. Appl.*, *1*, 399–429, 1991.
- Ritchie, J. T., D. C. Godwin, and S. Otter-Nache, *CERES-Wheat. A Simulation Model of Wheat Growth and Development*, Texas A&M Univ. Press, College Station, TX, 1988.
- Running, S. W., and J. C. Coughlan, A general model of forest ecosystem processes for regional application, I, Hydrologic balance, canopy gas exchange and primary production processes, *Ecol. Modell.*, *42*, 125–154, 1988.
- Segers, R., Methane production and methane consumption: A review of processes underlying wetland methane fluxes, *Biogeochemistry*, *41*, 23–51, 1998.
- Sellers, P. J., et al., BOREAS in 1997: Experiment overview, scientific results, and future directions, *J. Geophys. Res.*, *102*, 28,731–28,769, 1997.
- Shurpali, N. J., S. B. Verma, R. J. Clement, and D. P. Billesbach, Seasonal distribution of methane flux in a Minnesota peatland measured by eddy correlation, *J. Geophys. Res.*, *98*, 20,649–20,655, 1993.
- Shurpali, N. J., S. B. Verma, J. Kim, and T. J. Arkebauer, Carbon dioxide exchange in a peatland ecosystem, *J. Geophys. Res.*, *100*, 14,319–14,326, 1995.
- Sigren, L. K., S. T. Lewis, F. M. Fisher, and R. L. Sass, Effects of field drainage on soil parameters related to methane production and emission from rice paddies, *Global Biogeochem. Cycles*, *11*, 151–162, 1997.
- Silvola, J., J. Alm, U. Ahlholm, H. Nykanen, and P. J. Martikainen, CO<sub>2</sub> fluxes from peat in boreal mires under varying temperature and moisture conditions, *J. Ecol.*, *84*, 219–228, 1996.
- Skre, O., and W. C. Oechel, Moss functioning in different Taiga ecosystems in interior Alaska, *Oecologia*, *48*, 50–59, 1981.
- Suyker, A. E., S. B. Verma, R. J. Clement, and D. P. Billesbach, Methane flux in a boreal fen: Season-long measurement by eddy correlation, *J. Geophys. Res.*, *101*, 28,637–28,647, 1996.
- Suyker, A. E., S. B. Verma, and T. J. Arkebauer, Season-long measurement of carbon dioxide exchange in a boreal fen, *J. Geophys. Res.*, *102*, 29,021–29,028, 1997.
- Trettin, C. C., B. Song, M. F. Jurgensen, and C. Li, *Existing Soil Carbon Models do not Apply to Forested Wetlands*, USDA Forest Service GTR SRS-46, 2001.
- Valentine, D. W., E. A. Holland, and D. S. Schimel, Ecosystem and physical controls over methane production in northern wetlands, *J. Geophys. Res.*, *99*, 1563–1571, 1994.
- Verry, E. S., and N. R. Urban, Nutrient cycling at Marcell Bog, Minnesota, *Suo*, *43*, 147–153, 1992.
- Verseghy, D. L., CLASS - A Canadian land surface scheme for GCMs, I, Soil model, *Int. J. Climatol.*, *11*, 111–133, 1991.
- Walter, B. P., and M. Heimann, A process-based, climate-sensitive model to derive methane emissions from natural wetlands: Application to five wetland sites, sensitivity to model parameters, and climate, *Global Biogeochem. Cycles*, *14*, 745–765, 2000.
- Whiting, G. J., and J. P. Chanton, Primary production control of methane emission from wetlands, *Nature*, *364*, 794–795, 1993.
- Williams, T. G., and L. B. Flanagan, Measuring and modeling environmental influences on photosynthetic gas exchange in *Sphagnum* and *Pleuronium*, *Plant Cell Environ.*, *21*, 555–564, 1998.
- Yu, Z., I. D. Campbell, D. H. Vitt, and M. J. Apps, Modelling long-term peatland dynamics, I, Concepts, review, and proposed design, *Ecol. Modell.*, *145*, 197–210, 2001.
- Zheng, D., E. R. Hunt Jr., and S. W. Running, A daily soil temperature model based on air temperature and precipitation for continental applications, *Clim. Res.*, *2*, 183–191, 1993.
- Zoltai, S. C., R. M. Siltanen, and J. D. Johnson, *A Wetland Data Base for the Western Boreal, Subarctic, and Arctic Regions of Canada*, Inform. Rep. NOR-X-368, p. 30, Natural Resources Canada, Canada Forest Service, Northern Forestry Center, Edmonton, 2000.
- C. Li, Complex Systems Research Center, Institute for the Study of Earth, Oceans and Space, University of New Hampshire, Durham, NH 03824, USA.
- H. Li and C. C. Trettin, Center for Forested Wetlands Research, USDA Forest Service, 2730 Savannah Hwy., Charleston, SC 29414, USA.
- G. Sun, Southern Global Change Program, North Carolina State University, 920 Main Campus Dr. Venture II, Suite 300, Raleigh, NC 27606, USA.
- Y. Zhang, Environmental Monitoring Section, Canada Center for Remote Sensing, 588 Booth Street, Ottawa, Ontario, Canada K1A 0Y7. (yu.zhang@ccrs.nrcan.gc.ca)